CLASSICAL COHERENT RADIATION REACTION FOR MULTIPLE PARTICLES

A DISSERTATION SUBMITTED TO THE GRADUATE DIVISION OF THE UNIVERSITY OF HAWAIʻI AT MĀNOA IN PARTIAL FULFILLMENT OF THE REQUIREMENTS FOR THE DEGREE OF

DOCTOR OF PHILOSOPHY

IN

PHYSICS

DECEMBER 2014

BY

IAN HOWE

Dissertation Committee:

Luis Elias, Chairperson

John Madey

Eric Szarmes

John Learned

Magdy Iskander

Abstract

The unbounded radiated fields of point charges interfere constructively or destructively such that the total power radiated depends on the collective effects. By using the far field approximation for the radiated fields there is a unique assignment of partial power for each individual point charge in the collection. The unique assignment of partial power is a new development in classical electromagnetism, with potential applications beyond the Kimel-Elias approach to radiation reaction. The Kimel-Elias approach uses the partial power to find the radiation reaction for each point charge including the collective effects. This dissertation derives the uniqueness condition for the assignment of partial power and finds that the Kimel-Elias approach is only valid for highly relativistic point charges with nearly completely overlapping radiation fields. Examples of the Kimel-Elias approach are evaluated for two point charges in the cases of longitudinal and transverse acceleration, as well as for an undulator. The Kimel-Elias approach has never been implemented before and could potentially be used to explore the current problems simulations have with Free-Electron Laser (FEL) startup. In addition, a non-relativistic example is done with the partial power assignment using the Poynting vector and retarded time integrals, the results are nearly the same as those obtained numerically via the Feynman Wheeler absorber theory [1]. By using the partial power assignment the power radiated by individual particles in a non-relativistic system were found, the author is unaware of any other such development, the radiated power is always for the entire system.

Table of Contents

Table of Figures

Introduction

The contents of this thesis include a review of radiation reaction as applied to a single particle, followed by attempts to include multiple particles. Single particle radiation reaction is well understood, there are exact solutions that impose energy conservation in an ad hoc fashion or that do so by eliminating causality. As soon as another particle is included the results are no longer exact. Approximations are made to determine the retarded time and evaluate integrals.

The Kimel-Elias approach is an ad-hoc correction to the retarded theory of electromagnetism. The addition of advanced fields in the Feynman-Wheeler Absorber theory may provide a better theory of classical electromagnetism. However, the Kimel-Elias approach provides a model of radiation reaction that can be easily assimilated into a computer simulation. Whether the Feynman-Wheeler or retarded theory of radiation reaction results in a better understanding of real physical processes is not addressed in this thesis. It is sufficient that for a specific case the Kimel-Elias approach will do as advertised and conserve energy while the Liénard-Wiechert fields accurately portray the fields. To that end, this thesis is about discovering the restrictions on the Kimel-Elias approach that will allow for accurate modeling of classical point charges. Computer simulations of FEL and SASE startup would benefit from having the collective effects included in the codes. The startup of radiation by multiple particles in an undulator is a current problem that needs resolution.

Chapter 1 follows the historical time line of important progress on radiation reaction. It is not comprehensive, simply the work that has the most immediate bearing on the proceedings. For instance, Landau is left out; he pointed out that radiation reaction is so small for a single particle that it crosses over into the realm of quantum mechanics. Consequently, it can be ignored in classical electromagnetism and if it can't be ignored, you should be doing quantum

mechanics. Multiple particles can make this point moot by providing sufficient radiative power to make radiation reaction a non-ignorable classical effect.

Chapter 2 goes into detail on finding the radiation reaction for a single relativistic particle and explicitly demonstrates the traditional method that will be extended and used throughout the rest of the thesis. The traditional method involves finding the Liénard-Wiechert fields in unbounded space, calculating the instantaneous radiated power and then removing the energy from the kinetic energy of the particle. Chapter 2 continues with solving the equation of motion, this leads to some very disturbing conclusions outlined and interpreted by Dirac [2]. These conclusions are then embraced by Feynman and Wheeler and a consistent, although non-causal, theory is presented by them [3].

Chapter 3 provides the basis of the Kimel-Elias approach to radiation reaction for multiple particles [4]. I organized the presentation of partial powers according to my own scheme of partial Poynting vectors and discuss the possibility of alternate distributions of partial powers that were not considered as part of the Kimel-Elias paper [4]. Then show that with the far field approximation the partial power is unique, a feature that was not considered in the original paper. In addition, the presentation of the partial power here makes it clear that it is not restricted for use solely with the Kimel-Elias approach.

Chapter 4 discusses the Kimel-Elias approach by examining its application in examples, the Kimel-Elias approach has never been implemented before and requires some analysis to determine when and how to apply it. The first example of the Kimel-Elias approach is an original and very detailed example of radiation reaction from two point charges in a linear acceleration burst. The radiation reaction is found in two ways; the direct, and ad hoc, imposition of energy conservation via retarded time integrals, and by application of the Kimel-

Elias approach. The methods are then compared and the Kimel-Elias approach is shown to be equivalent for this particular example. Also appearing in chapter 4 is the definition of coherent as being equivalent to interference in a classical situation. The case of synchrotron radiation is briefly discussed as an instance where the Kimel-Elias approach is not ideal because of the condition required to have overlapping radiation. As a result, the Kimel-Elias approach is shown to have definite and restrictive conditions; highly relativistic point charges and overlapping radiated fields. An original example of one-dimensional spontaneous emission in an undulator is also included; this could be extended to model startup in an FEL or SASE radiation, a fundamental problem that still seeks resolution.

Chapter 5 explores an original derivation of radiation reaction by two point charges undergoing non-relativistic dipole radiation. This ties into current work by John Madey, Pardis Niknejadi and Jeremy Kowalczyk on the application of the Feynman-Wheeler absorber theory to multiple particles [1], and it shows that the two approaches broadly agree. This non-relativistic example also compliments the highly relativistic example in chapter 4 and shows the differences between them. The introduction of partial power into this derivation represents a new approach to evaluating the power of systems of particles.

Appendix I summarizes some experimental work that has or could take place here at the University of Hawai‘i. Transition radiation from the Mark III FEL diagnostic beam line could be used to determine the bunch length of the electron pulses from the transition of coherent to incoherent radiation [5]. Actual measurements of the energy radiated due to transition radiation were made in order to determine that it is feasible to use transition radiation to measure the bunch length and explore the transition from coherent to incoherent radiation. Theoretical estimates of the power output from synchrotron radiation were made for the Mark

III FEL to show that it is also feasible to use Synchrotron radiation to explore coherence in the THz domain.

The appendix has an original derivation of the unbounded Green function solution to the wave equation. Traditionally the Fourier transform is applied to (7.3) , I have never seen it applied to (7.1) and (7.2) before, although it seems like someone should have done it before. However, by doing so a long standing issue that calls into question the validity of solutions to (7.3) in curvilinear coordinates is resolved, at least for the potentials but not for the fields.

Chapter 1. Radiation Reaction Background

Maxwell's equations determine the electric and magnetic fields given the source. The effect the fields have on the source is still not fully understood. In particular, the energy is not conserved when the sources are radiating. The usual solution is to impose an ad hoc force on the radiating source to ensure energy conservation. The added force is referred to as radiation reaction. For a single particle with absorbing boundary conditions, the radiation reaction force is well known. For multiple particles radiating collectively, the radiation reaction force is not known. [6]

While the true dynamical equation of motion for a point charge would be of great benefit to classical electromagnetism as well as quantum mechanics. There is doubt as to what the true dynamical equation of motion would be. The leading candidate is the Lorentz-Dirac equation which contains the Lorentz force and added to that is the relativistic radiation reaction of a single point charge. [7]

The Lorentz-Dirac equation conserves energy for a single particle but the solution of this dynamical equation contains exponential runaways. Since charged particles do not simply speed off to infinity due to spontaneous radiation, a fix was considered that allowed pre-acceleration. The point charge would accelerate in preparation to be accelerated by the radiation reaction to sufficiently cancel the exponential motion. For those that were fond of causality this violation (although immeasurable due to the expected pre-acceleration occurring around 10^{-23} seconds before the acceleration due to radiation [8]) was unacceptable, no alternative theory has been forthcoming, however prescriptions for the conservation of energy and momentum are used without alteration of the concept of causality.

For a single particle, Quantum-Electrodynamics (QED) has been remarkably successful and can be counted as the true description of electromagnetism. While QED conserves energy, infinites in the self-energy which occur in the classical theory also carry over to the quantum realm. For a 4-dimensional space-time QED is renormalizable and the infinities are unpleasant but manageable. In the classical theory the infinities are often ignored as well, however, before renormalization was hit upon, there were attempts to resolve the infinities the classical theory in the hopes that the quantized version would no longer have infinities either. A notable example is the absorber theory of Feynman and Wheeler.

In the absorber theory of Feynman and Wheeler causality is abandoned in favor of a holistic philosophy that resolves some seemingly contradictory observations of classical electromagnetism. These observations are; (1) Maxwell's equations are time symmetric which allows for retarded and advanced solutions, (2) experiments have borne out causality over and over again, and (3) Dirac showed that the relativistic radiation reaction term can be recovered by a suitable limiting procedure involving the difference of the retarded and advanced solutions to Maxwell's equations. [9] The resolution of these facts lies in the identification of the radiated fields as a time symmetric combination of the advanced and retarded solutions and the realization that the difference in the retarded and advanced solutions is time anti-symmetric and so must be coming from an external source. Feynman and Wheeler identify this external source as the absorbers [3]. The satisfaction that can be derived from this theory is of a meta-physical nature as the superposition of the radiated fields of the source and the advanced fields travelling backward in time from the absorbers produce the full retarded solution that is observed by experiment and the force on the source is mathematically identical to the Lorentz-Dirac equation. Consequently, for a single particle, the Feynman-Wheeler theory is mathematically identical to the previous theory but the way in which it is thought about is

consistent and not ad hoc. Since the differences with the previous theory are conceptual and no discernible difference is detectable in the dynamical equation from which a quantum theory would be quantized, the absorber theory has been considered a theoretical oddity rather than a viable and robust description of a point charge that is more consistent than the standard view.

Consequently we have in Classical Electromagnetism a set of equations that govern the interaction of charged particles via electric and magnetic fields that does not quite work in a self-consistent way. The magnitude of the radiation reaction force is so small that in almost all classical situations it is negligible so that Classical Electromagnetism is sufficient to describe the phenomena (When Rohrlich discovered that Landau made note of this he published a 3rd edition of his book to cover this topic [8]). An important exception occurs in the case of SASE (self-amplified spontaneous emission) radiation from an electron beam comprised of many electrons. If the initial electron beam is bunched so as to suppress the stimulated radiation then the coherent emission is quite large and sensitive to the distribution of the particles, therefore the radiation reaction term, while still fairly small, is required to find the motion of the electrons that is accurate enough to correctly predict the radiation. Computer programs are written that impose energy conservation on the particles and iteratively find the motion and the subsequent radiation. The basis for these programs can be fairly simple (requiring many iterations) or more robust (requiring fewer iterations). Since the more robust programs are preferred, there is theoretical work done to advance Classical Electromagnetism as far as possible towards a self-consistent energy conserving theory. [4] [9]

Chapter 2. Conservation of Radiated Energy for a Single Particle

The dynamic equation for a point charge is usually dominated by the Lorentz force

$$\vec{F} = q\left(\vec{E} + \vec{v} \times \vec{B}\right),$$

where the electric and magnetic fields are usually considered to be external fields not created by the point charge itself. Now consider the differential work done on the point charge

$$dW = \vec{F} \cdot d\vec{x},$$

now divide by the differential time to find the power

$$P = \frac{dW}{dt} = \vec{F} \cdot \frac{d\vec{x}}{dt} = \vec{F} \cdot \vec{v} = q\vec{E} \cdot \vec{v}\ .$$

The power put into or extracted from the point charge is a dot product of the external electric field and the velocity of the point charge (or it could be considered the current density). This is sufficient so long as the point charge does not radiate.

Consider a point charge in a vacuum with absorbing boundary conditions that is undergoing acceleration. It is possible to find the power radiated by this point charge without specifying the cause of the acceleration. To do this start with the Liénard-Wiechert electric field

(2.1) $$\vec{E} = \frac{q}{4\pi\varepsilon_0}\left[\frac{\hat{n} - \vec{\beta}}{\gamma^2 R^2\left(1 - \hat{n}\cdot\vec{\beta}\right)^3} + \frac{\hat{n} \times \left\{\left(\hat{n} - \vec{\beta}\right) \times \vec{\alpha}\right\}}{cR\left(1 - \hat{n}\cdot\vec{\beta}\right)^3}\right]_{\text{retarded}}.$$

The motion of the point charge completely specifies the fields created by the point charge; at the same time the fields radiated by the point charge affect its motion through energy and momentum conservation. At this point the acceleration and the velocity are unknown. A spherical surface of very large radius with its center coincident on the instantaneous retarded

position of the point charge is chosen to find the power passing through this surface. The Poynting vector is given by

$$\vec{S} = \frac{1}{\mu_0}\vec{E}\times\vec{B} = \frac{1}{\mu_0}\vec{E}\times\left(\hat{n}\times\vec{E}\right) = \frac{1}{\mu_0}E^2\hat{n},$$

where the unit vector is the radial unit vector. Since the surface is so far away the far-field approximation can be made. The first term in (2.1) is the velocity field and the second is the radiation or acceleration field. Keeping only the acceleration field the electric field becomes

(2.2) $$\vec{E} = \frac{q}{4\pi\varepsilon_0 c}\frac{[\alpha]}{\left[R(1-\hat{n}\cdot\vec{\beta})^3\right]}\left[\hat{n}\times\left\{(\hat{n}-\vec{\beta})\times\hat{e}_\alpha\right\}\right],$$

where the normalized acceleration was split into a magnitude and a unit vector. If the choice of coordinates is such that the retarded normalized velocity is along the z-axis then the two unit vectors can be represented as

$$\begin{aligned}\hat{n} &= \hat{e}_x\sin\theta\cos\phi + \hat{e}_y\sin\theta\sin\phi + \hat{e}_z\cos\theta \\ \hat{e}_\alpha &= \hat{e}_x\sin\psi\cos\Gamma + \hat{e}_y\sin\psi\sin\Gamma + \hat{e}_z\cos\psi\end{aligned}.$$

The power passing through the arbitrary surface in terms of the retarded time is

(2.3) $$P = \int\vec{S}\cdot\hat{n}dA\left[1-\hat{n}\cdot\vec{\beta}\right] = \frac{1}{\mu_0 c}\int_0^{2\pi}\int_0^{\pi}E^2\left[R^2\left(1-\hat{n}\cdot\vec{\beta}\right)\right]\sin\theta d\theta d\phi.$$

The vector $\hat{e}_\alpha$ is a constant in the integration, yet the expansion into Cartesian coordinates in terms of the angle the acceleration makes with the velocity, ψ, and the azimuthal angle the acceleration is canted by, Γ, is useful. The triple cross product in (2.2) is simplified by the BAC-CAB rule

(2.4) $$\left[\hat{n}\times\left\{\left(\hat{n}-\vec{\beta}\right)\times\hat{e}_\alpha\right\}\right] = \left(\hat{n}-\vec{\beta}\right)\hat{n}\cdot\hat{e}_\alpha - \left(1-\hat{n}\cdot\vec{\beta}\right)\hat{e}_\alpha.$$

The power in (2.3) when combined with (2.2) and (2.4) becomes

$$P=\frac{q^2\left[\alpha^2\right]}{\left(4\pi\right)^2\varepsilon_0 c}\int_0^{2\pi}\int_0^{\pi}\frac{\left(1-2\hat{n}\cdot\vec{\beta}+\beta^2\right)\left(\hat{n}\cdot\hat{e}_\alpha\right)^2-2\left(1-\hat{n}\cdot\vec{\beta}\right)\left(\hat{n}\cdot\hat{e}_\alpha\right)\left(\hat{n}\cdot\hat{e}_\alpha-\hat{e}_\alpha\cdot\vec{\beta}\right)+\left(1-\hat{n}\cdot\vec{\beta}\right)^2}{\left(1-\hat{n}\cdot\vec{\beta}\right)^5}\sin\theta d\theta d\phi$$

.

The dot products then give

$$\begin{aligned}\hat{n}\cdot\hat{e}_\alpha&=\cos\theta\cos\psi+\cos\left(\Gamma-\phi\right)\sin\theta\sin\psi\\ \hat{n}\cdot\vec{\beta}&=\beta\cos\theta\\ \hat{e}_\alpha\cdot\vec{\beta}&=\beta\cos\psi\end{aligned}\quad .$$

Using Mathematica to integrate over the angles leaves the Liénard result

(2.5) $$P=\frac{q^2\left[\alpha^2\right]}{6\pi\varepsilon_0 c}\left[\gamma^6\left(1-\beta^2\sin^2\psi\right)\right].$$

The power is proportional to the acceleration squared. When the acceleration is parallel to the velocity the power is proportional to γ^6 and when the acceleration is perpendicular to the velocity it is proportional to γ^4. This is the amount of power being radiated instantaneously by the point charge. Coordinate free notation can be reinserted into (2.5) by exploiting the vector nature of the normalized acceleration and velocity

(2.6) $$P=\frac{q^2\gamma^6}{6\pi\varepsilon_0 c}\left[\left|\alpha\right|^2-\left|\vec{\beta}\times\vec{\alpha}\right|^2\right].$$

This energy loss can be implemented in the dynamics of the particle through the use of energy conservation

(2.7) $$\frac{dU}{dt}=mc^2\frac{d\gamma}{dt}=q\vec{E}\cdot\vec{v}-P\,,$$

where P is given by (2.6) and the electric field is the external electric field. When (2.7) is expressed as a force equation it is called the Lorentz-Dirac equation, (2.7) is recovered by taking the dot product of the Lorentz-Dirac equation with velocity. The equation (2.7) is non-linear in $\vec{E}$.

(2.7) was solved by Dirac [2] for the motion of an electron without an incident field, and given some initial acceleration. Starting with the alternative form

$$\frac{3m}{2e^2}\dot{v}_\mu - \ddot{v}_\mu - \dot{\bar{v}}^2 v_\mu = 0, \tag{2.8}$$

where Gaussian units (and $c = 1$) were used and the equation is written in terms of the four vector velocity. Dirac then noted that the second term in (2.8) makes this a third order equation requiring three initial conditions instead of the usual two and then simplified the equation by choosing the initial velocity and acceleration to be in the x-direction. (2.8) then simplifies to

$$\frac{3m}{2e^2}\ddot{x} - \dddot{x} + \frac{\dot{x}\ddot{x}^2}{1+\dot{x}^2} = 0. \tag{2.9}$$

Dirac then divided by the acceleration $\ddot{x}$ then integrated twice choosing his origin such that the first constant of integration is $-\ln\left(\frac{3m}{2e^2}\right)$. The result is that

$$\begin{aligned} \dot{x} &= \sinh\left(e^{\frac{3m}{2e^2}s} + b\right) \\ \dot{t} &= \cosh\left(e^{\frac{3m}{2e^2}s} + b\right) \end{aligned},$$

where b is the second constant of integration and s is the distance from the origin in the x-direction. As s increases the velocity approaches the speed of light very rapidly; not what one would expect of an electron. This lead Dirac to conclude:

"We must obtain solutions of our equations of motion for which the initial position and velocity of the electron are prescribed, together with its final acceleration, instead of solutions with all the initial conditions prescribed." [2]

By applying the three boundary conditions as described by Dirac the runaway solution of (2.9) will be avoided but the initial acceleration of the electron is found to occur before the electron is disturbed. Dirac then concludes that there is either a pre-acceleration on the time scale of $2e^2/3m$ or the electron has a radius of the order $2e^2/3m$. When divided by the speed of light twice this gives a radius of the order 1.87×10^{-13} cm; when divided by the speed of light three times it gives the time scale 6.24×10^{-24} sec. The classical electron radius is of the same order as the one quoted above; therefore, quantum theory is needed to describe what happens at this scale. QED models of contact interactions for $e^+e^- \to \gamma\gamma(\gamma)$ infer that the radius of the electron must be smaller than 1.17×10^{-19} m [10]. Therefore pre-acceleration is required at a time scale so short that it cannot be measured.

Feynman and Wheeler advanced Dirac's work by embracing the non-causality to such an extent that radiation is seen as an exchange of radiation between the emitter and absorber in both directions of time [3]. The wave equation has two possible solutions the advanced and the retarded, indicating that radiation from a particle can arrive at a point in space from the past traveling forward in time (retarded) or from the future traveling backwards in time (advanced). For Feynman and Wheeler the emitter radiates a symmetric combination of advanced and

retarded fields, these fields do not act on the particle that emits them. The absorber is introduced to impose boundary conditions on the wave equation. When the radiation reaches the absorber, the absorber will emit retarded and advanced fields. The advanced field from the absorber will travel backwards in time to the emitter and cause the radiation reaction in the emitter at the time of emission. Feynmann and Wheeler found that the advanced field of the absorber can be expressed as the anti-symmetric combination of the advanced and retarded fields of the emitter. The calculation of radiation reaction for that exact combination has already been done by Dirac. In the rest of space the combination of the advanced fields of the absorber with the radiated fields, both advanced and retarded, will be in terms of the field strength tensor,

$$F^{\mu\nu} = \frac{1}{2}\left(F_{adv}^{\mu\nu} + F_{ret}^{\mu\nu}\right) + \frac{1}{2}\left(F_{ret}^{\mu\nu} - F_{adv}^{\mu\nu}\right) = F_{ret}^{\mu\nu}\ , \tag{2.10}$$

which is the full retarded field in complete accord with experiment. The emitter radiates backwards and forwards in time. The advanced field from the absorber travels backwards in time; to an observer that has a memory of the past but none of the future, the advanced field appears to propagate instantaneously and acts on the emitter at the exact time that it emits, seemingly instantaneous action at a distance. Feynman and Wheeler then derive radiation reaction utilizing the absorber model, in four different ways. The first derivation involves a nonrelativistic charge that is somehow accelerated. The radiated field from the particle is taken to be the retarded solution of Maxwell's equation with the velocity field dropped. The absorber is taken to be a spherically symmetric collection of charges (of charge e_k and mass m_k). In order to properly consider the collective effect of the absorber on the source, the effect on the phase of the advanced field from propagating through a medium must be included. To do this the frequency domain is then invoked and frequency dependent index of refraction

$$n = 1 - \frac{2\pi N e_k^2}{m_k \omega^2}$$

is used to find the phase lag of the advanced field when it reaches the source. The result is that the nonrelativistic radiation reaction force is 90° out of phase with the acceleration which allows the force to be expressed in a form that is independent of the frequency

(2.11) $$F_{\text{total reaction}} = \frac{2e^2}{3c^3}\left(-i\omega a\right) = \frac{2e^2}{3c^3}\frac{da}{dt}$$

in Gaussian units. The second derivation, still nonrelativistic, clears up the use of the full retarded solution of Maxwell's equations to find the motion of the absorber particles by summing the advanced fields from all the absorbers to show that (2.10) will result in the vicinity of the source. The result is that the absorbers produce an electric field in the vicinity of the source that is expressed in terms of quantities associated with the source as

(2.12) $$E_{radreac} = \frac{2e}{3c^3}\left(-i\omega a\right)e^{-i\omega t}\left[\frac{\sin u}{u} - P_2\left(\cos\left(\vec{a},\vec{r}\right)\right)\left(\frac{\sin u}{u} - \frac{3\sin u}{u^3} + \frac{3\cos u}{u^2}\right)\right],$$

where $u \equiv \frac{\omega r}{c}$ and $P_2\left(\cos\left(\vec{a},\vec{r}\right)\right)$ is the Legendre polynomial with the cosine of the angle between the acceleration and the field point vector (source at the origin) as the argument. When multiplied by e and evaluated at $r = 0$ the result is (2.11). A number of wavelengths from the source, (2.12) will turn into half the difference of the retarded and advanced fields found from Maxwell's equations for the source. What happens between $r = 0$ and a number of wavelengths from the source is left unexplored by Feynman and Wheeler. John Madey has proposed that the application of (2.12) to multiple source particles close to each other will provide a correct description of partially coherent radiation reaction. [1]

The third and fourth derivations are for relativistic motions. The third approach is largely the same as the first but mathematically more intimidating. The main result is that radiation reaction for a single particle is independent of the properties of the absorber so long as it is completely absorbing. This conclusion motivates the fourth derivation which utilizes physical arguments to find that the fields experienced by a charge (the jth charge) inside a complete absorber are

$$\sum_{k \neq j} F_{ret}^{(k)} + \frac{1}{2}\left(F_{ret}^{(j)} - F_{adv}^{(j)}\right).$$

The first term corresponds to the Lorentz force and the second term to the radiation reaction force.

Chapter 3. Radiated Power for Multiple Particles

One way to impose energy conservation is to impose it ad hoc. By finding the radiated energy and subtracting that from the particle energy; energy is conserved. This is what was done in chapter 2 for a single particle, for N particles the Poynting vector becomes

$$\vec{S} = \frac{1}{\mu_0}\left(\sum_{j=1}^{N}\vec{E}_j\right)\times\left(\sum_{k=1}^{N}\vec{B}_k\right). \tag{3.1}$$

The Poynting vector has no physical interpretation when evaluated at a single point, it requires a flux through an area or a volume integration to acquire physical meaning. For the sake of clarity and brevity the following discussion involving the Poynting vector will concentrate on the Poynting vector instead of the flux of the Poynting vector through a closed surface. However, taking the flux of the Poynting vector allows for the interpretation of power radiated from the distribution as well as partial power.

For Liénard-Wiechert fields the electric and magnetic fields are related by

$$\vec{B} = \frac{[\hat{n}]_{ret}\times\vec{E}}{c},$$

where $[\hat{n}]_{ret}$ is the direction from the retarded position of the source to the field point. The summations can be done after the cross product because of the associative properties of multiplication, making (3.1)

$$\vec{S} = \frac{1}{\mu_0 c}\sum_{j=1}^{N}\sum_{k=1}^{N}\vec{E}_j\times\left([\hat{n}_k]_{ret}\times\vec{E}_k\right) = \frac{1}{\mu_0 c}\sum_{j=1}^{N}\sum_{k=1}^{N}\left([\hat{n}_k]_{ret}\left(\vec{E}_j\cdot\vec{E}_k\right)-\vec{E}_k\left([\hat{n}_k]_{ret}\cdot\vec{E}_j\right)\right). \tag{3.2}$$

There is nothing special about the labels j and k, so they can be interchanged without affecting the total Poynting vector. The Poynting vector can be expressed as a sum of N terms by

$$\vec{S} = \sum_{j=1}^{N} \vec{S}_j$$

(3.3)

$$\vec{S}_j \equiv \frac{1}{\mu_0 c} \sum_{k=1}^{N} \left(\left[\hat{n}_k \right]_{ret} \left(\vec{E}_j \cdot \vec{E}_k \right) - \vec{E}_k \left(\left[\hat{n}_k \right]_{ret} \cdot \vec{E}_j \right) \right).$$

The partial Poynting vector $\vec{S}_j$ is then interpreted as the Poynting vector emanating from the jth particle. This allows for the identification of energy loss of individual particles rather than the system as a whole. However, if j and k are interchanged an equally valid assignment for $\vec{S}_j$ is

(3.4)

$$\vec{S}_j \equiv \frac{1}{\mu_0 c} \sum_{k=1}^{N} \left(\left[\hat{n}_j \right]_{ret} \left(\vec{E}_j \cdot \vec{E}_k \right) - \vec{E}_j \left(\left[\hat{n}_j \right]_{ret} \cdot \vec{E}_k \right) \right).$$

These two equations can be very easily interpreted if the magnetic field is reintroduced as

(3.5)

$$\vec{S}_j = \frac{1}{\mu_0} \vec{E}_j \times \left(\sum_{k=1}^{N} \vec{B}_k \right)$$
$$\vec{S}_j = \frac{1}{\mu_0} \left(\sum_{k=1}^{N} \vec{E}_k \right) \times \vec{B}_j ,$$

where the top equation of (3.5) corresponds to (3.3) and the bottom is equivalent to (3.4). The Kimel-Elias approach uses the upper equation in (3.5) without consideration of any other possibility [4]. This presents a challenge for the stated interpretation since the assigned energy loss for the individual particles is not unique. If $\left[\hat{n}_j \right]_{ret} \approx \left[\hat{n}_k \right]_{ret}$ for all values of j and k then the two assignments of (3.5) will be the same and converge to

(3.6)

$$\vec{S}_j = \frac{1}{\mu_0 c} \sum_{k=1}^{N} \left[\hat{n} \right]_{ret} \left(\vec{E}_j \cdot \vec{E}_k \right).$$

Other assignments of the partial Poynting vector will also converge to (3.6) as demonstrated by applying the same restriction to (3.2) so that

$$\vec{S} = \frac{1}{\mu_0 c}\sum_{j=1}^{N}\sum_{k=1}^{N}\left(\left[\hat{n}_k\right]_{ret}\left(\vec{E}_j \cdot \vec{E}_k\right) - \vec{E}_k\left(\left[\hat{n}_k\right]_{ret} \cdot \vec{E}_j\right)\right) \approx \frac{1}{\mu_0 c}\sum_{j=1}^{N}\sum_{k=1}^{N}\left[\hat{n}\right]_{ret}\left(\vec{E}_j \cdot \vec{E}_k\right).$$

No matter how the summation is divided up (3.6) will result. However, to make the interpretation that the $\vec{S}_j$ vector corresponds to the jth particle, only the two definitions given in (3.5) can apply. The main difficulty in assigning individual power to particles from the total power radiated by all the particles is the absence of phase information in the total power. The phase information is lost when those fields are superposed. Consequently, by choosing either one of (3.5) the phase information of particle j is preserved.

For $\left[\hat{n}_j\right]_{ret} \approx \left[\hat{n}_k\right]_{ret}$ to be valid, the point of observation has to be much farther from the particles than the retarded distance between the particles, $\left[R\right] \gg \gamma^2 d$, where $\gamma^2 d$ is a generous estimate of possible retarded distances between the particles given the present time distance between the particles, d. The individual power of the jth particle is then

(3.7) $$P_j(t_j) = \oint\left[1 - \hat{n}\cdot\vec{\beta}_j\left(t_j\right)\right]\vec{S}_j\left(t\right)\cdot d\vec{A},$$

where the power is evaluated at the retarded time of particle j. The quantity in square brackets relates the present time at the location of the closed surface to the retarded time of particle j. The partial Poynting vector in (3.7) is given by (3.6) and is in terms of the retarded times of all particles. Presuming that the position of a particle at the present time is known; then the retarded time is the time it takes for light to travel from where it was radiated to the point of observation at the coincident present time, the particle moving from where it radiated to its

present position at the same time. This leads to an equation for the retarded time that is, in general, transcendental

$$t = t_j + \frac{R(t_j)}{c}, \tag{3.8}$$

with $R(t_j)$, the retarded distance for particle j, being a function of the retarded time for particle j. Taking the differential of (3.8) is what leads to the square brackets in (3.7)

$$dt = dt_j + \frac{dR}{c} = dt_j + \frac{1}{c}\vec{R}\cdot\nabla R = dt_j\left(1 - \frac{1}{c}\hat{n}\cdot\vec{v}_j\right).$$

The gradient of R is over the source coordinates, while the field point is fixed, giving rise to minus the velocity of particle j.

The retarded time for the light to travel from the position of the particle to the surface where the Poynting vector is to be evaluated is, in general, not the same whether it is for different particles when looking at a single surface element or for the same particle at different points on the surface.

Partial power is uniquely assignable when the far field approximation is used. This means that the phase information can be preserved and the point charges will be, in principle, distinguishable. This was not known to be the case previously and is a very important contribution to classical electromagnetism. The only approximation used is the far field approximation, so that this result is more broadly applicable than just for the Kimel-Elias approach. It is, however, formulated for the retarded theory of electromagnetism; further work would be required to find partial power assignments for the Feynman-Wheeler Absorber theory.

Chapter 4. Kimel-Elias Approach to Radiation Reaction

The Kimel-Elias approach is based upon the previous discussion of partial power assignments specifically for free electrons. The partial power per unit solid angle for the jth electron is given by

$$\frac{dP_j\left(t,t_j'\right)}{d\Omega}=\varepsilon_0 cR^2\left|\vec{E}_j\left(t,t_j'\right)\cdot\left[\sum_k \vec{E}\left(t,t_k'\right)\right]\right|_{ret},$$

where t' is the retarded time [4]. The instantaneous change in electron energy for the jth electron is then found by using the Liénard-Wiechert fields with the further assumption that the differences in the retarded times leave the distance and angle from the retarded position to the observation approximately the same for all electrons. The only difference between the radiation from the different electrons is then found to be the phase shift caused by the different retarded times. This assumption is consistent with the far field assumption that the observation point is very far from all the charges and does not require that all the charges be located at the same place. Consequently, in the following equation the retarded times are retarded with respect to the surface element but the time has been rescaled with respect to particle j,

$$\left[\frac{d\gamma_j(t)}{dt}\right]=-\frac{2r_e\gamma^4}{3c}\sum_k\left[\gamma^2\alpha_{jp}\left(t\right)\alpha_{kp}\left(t_k\right)+\vec{\alpha}_{j\perp}\left(t\right)\cdot\vec{\alpha}_{k\perp}\left(t_k\right)\right]_{\text{ret}}.$$

Here, the time has been redefined to make the retarded time of particle j equal to t and the time t_k is the retarded time for the kth particle, which has also been shifted by the same amount as the retarded time for particle j. [4] However, there is ambiguity here as the retarded time is defined to a single point on the surface while the results provided above have already been

integrated around the closed surface. So to what point are the retarded times of the kth particle retarded?

Highly relativistic particles radiate directionally with most of the radiation focused towards the same direction as the velocity of the particle. This can allow for a good approximation of the radiated power by integrating over a small area instead of an entire closed surface. In addition to simplifying the integration, this approximation can also simplify the calculations of retarded time since the field point will vary only slightly. In particular, a linear filamentary arrangement of highly relativistic electrons will have retarded times that can be described one-dimensionally (due to the combination of having the electrons line up and point towards the field point) and thus solved easily.

The process that takes account of radiation reaction is an iterative one. First the motion of the particles are found without considering the effect of radiation, this is the zeroth order approximation of the particles motion, $\vec{F} = q\left(\vec{E}_{\text{External}} + \vec{v} \times \vec{B}_{\text{External}}\right)$. Then the Liénard-Wiechert fields are found from the motion of the particles. At this point the energy radiated can be determined and removed from the particles in an ad hoc fashion in order to find the motion a second time, $\frac{dU}{dt} = \vec{E} \cdot \vec{J} - \text{Rad. Reac.}$. This in turn affects the radiated fields, which adjusts the energy radiated and the motion of the particles. This can be done iteratively until the subsequent adjustments are as small as desired. When this occurs, the motion of the particles and the electric and magnetic fields should be accurately but approximately described.

In the following examples the number of particles considered will be two, except for the first example. If the interaction of two particles is understood then the number of particles can be extended to an arbitrary amount without much difficulty. The main purpose of the examples

is to explore the Kimel-Elias approach to coherent radiation reaction and any restrictions to the application of the Kimel-Elias approach. No examples were worked nor any limitations considered in the Kimel-Elias paper [4].

Example 1: A linear acceleration burst for one particle

To set up the discussion of two particles, first consider a brief acceleration applied in the direction of motion of a point charge, q. This example was used in Zangwill [6] in order to find the radiation spectrum. Assuming a square-pulse acceleration burst in unbounded vacuum

$$a(t) = \frac{\Delta v}{\Delta t}\left\{\Theta(t) - \Theta(t - \Delta t)\right\},$$

where the change in particle velocity is Δv and the time duration of the square-pulse is Δt. The retarded time is found from figure 1 below. By looking at the vertical and horizontal components there are two equations

$$\begin{aligned} R\cos\theta + [z] &= [R]\cos\psi \\ R\sin\theta &= [R]\sin\psi \end{aligned},$$

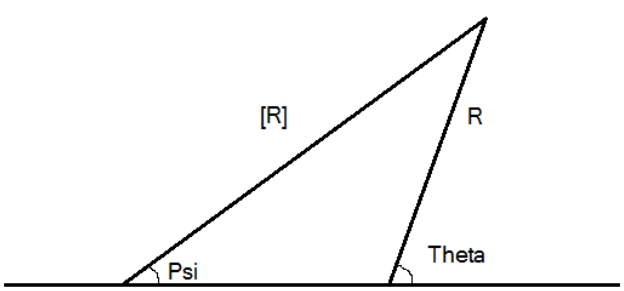

Figure 1: The present and retarded position of a point charge with respect to the point of observation.

where $[R] = c(t - t_r)$ and $[z] = \int_{t_r}^{t} v(t')dt'$. If the speed is given by v_0 before the acceleration and reaches a final constant speed after the acceleration then the only time the point charge will radiate is during the acceleration, so the retarded times of interest occur between $0 \le t_r \le \Delta t$. Assuming

the time of acceleration as well as the magnitude of acceleration to be very small the speed can be approximated as

$$v(t) = v_0\Theta(-t) + \bar{v}\left\{\Theta(t) - \Theta(t-\Delta t)\right\} + v_f\Theta(t-\Delta t)\ ,$$

where $\bar{v} \equiv v_0 + \Delta v/2$ and $v_f \equiv v_0 + \Delta v$. The retarded distance is then found by integrating the speed, with the restriction that the retarded time is larger than zero but smaller than Δt,

$$\begin{aligned}
[z] &= \frac{\bar{v}[R]}{c}\left\{\Theta(t) - \Theta(t-\Delta t)\right\} \\
&+ \left(\left\{v_f - \bar{v}\right\}(t-\Delta t) + \frac{\bar{v}[R]}{c}\right)\left\{\Theta(t-\Delta t) - \Theta\left(t - \frac{[R]}{c} - \Delta t\right)\right\}. \\
&+ \frac{v_f[R]}{c}\Theta\left(t - \frac{[R]}{c} - \Delta t\right)
\end{aligned} \tag{4.1}$$

To find an expression for $[R]$ consider that this expression is equivalent to $[z] = a + b[R]$, where

$$\begin{aligned}
a &= \frac{\Delta v}{2}(t-\Delta t)\left\{\Theta(t-\Delta t) - \Theta(t-\Delta t - \frac{[R]}{c})\right\} \\
b &= \frac{\bar{v}}{c}\left\{\Theta(t) - \Theta(t-\Delta t)\right\} + \frac{\bar{v}}{c}\left\{\Theta(t-\Delta t) - \Theta(t-\Delta t - \frac{[R]}{c})\right\} + \frac{v_f}{c}\Theta(t-\Delta t - \frac{[R]}{c})
\end{aligned}.$$

Here b changes very little as a function of time and $a \ll R$ so that a can be neglected. Consequently, $b \approx \bar{\beta}$ for all times of interest and the retarded distance is found from

$$\begin{aligned}
R\cos\theta + \bar{\beta}[R] &= [R]\cos\psi \\
R\sin\theta &= [R]\sin\psi
\end{aligned}.$$

Eliminate ψ by squaring both equations and adding, then

$$[R]^2(1-\bar{\beta}^2)-2\bar{\beta}R\cos\theta[R]-R^2=0\,.$$

By the quadratic formula

(4.2) $$[R]=\bar{\beta}\bar{\gamma}^2\cos\theta R+\bar{\gamma}^2R\sqrt{\bar{\beta}^2\cos^2\theta-\left(1-\bar{\beta}^2\right)}\,.$$

For a highly relativistic particle, (4.2) can be approximated as

$$[R]\approx 2\bar{\gamma}^2\cos\theta R\,.$$

The results from Zangwill [6] when applied to a highly relativistic point charge show an angular emission of radiated power that looks like

(4.3) $$\frac{dP}{d\Omega}\approx\frac{2\mu_0q^2a^2}{\pi^2c}\frac{\bar{\gamma}^8\left(\bar{\gamma}\psi\right)^2}{\left(1+\left(\bar{\gamma}\psi\right)^2\right)^5}\,,$$

for small angles as well. Plotted in Mathematica, the graph of the angular distribution (4.3), where $\gamma=10$ was used as larger values of γ make the distribution even closer to the axis and hard to see. Figure 2 shows a hollow cone of radiation directed along the direction of motion which is coincident with the acceleration. No radiation is emitted in the exact direction of acceleration, but the peak radiated power occurs at $\psi_{\text{peak}}=\pm\frac{1}{2\bar{\gamma}}$. Each of the lobes have an angular spread of $\frac{1}{\bar{\gamma}}$, meaning that a majority of the radiated power is emitted within $\psi_{\max}\sim\frac{1}{\bar{\gamma}}$ which is very close to the velocity axis. The peak power at ψ_{peak} goes as $\bar{\gamma}^8$. The total

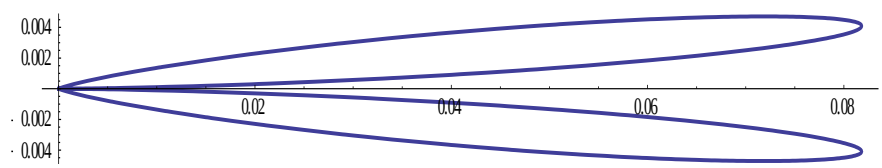

Figure 2: The angular distribution of radiated power for a single particle with coincident velocity and acceleration.

instantaneous radiated power without approximation is given by (2.6) and goes as $\bar{\gamma}^6$. The radiation spectrum is then found from the approximate motion of the point charge and

$$\frac{dI(\omega)}{d\Omega} \approx \frac{\mu_0 q^2}{16\pi^3 c}\left|\frac{\hat{n}\times(\hat{n}\times\Delta v)}{\left(1-\vec{\bar{\beta}}\cdot\hat{n}\right)^2 \Delta t}\int_0^{\Delta t} d\tau e^{i\omega\left(1-\hat{n}\cdot\vec{\bar{\beta}}\right)\tau}\right|^2, \tag{4.4}$$

where τ is the retarded time. (4.4) is not a direct Fourier transform of the exact version of (4.3) because the transition from present time to retarded time is made once in (4.3) but it is made twice in (4.4), so that after integrating and squaring

$$\frac{dI(\omega)}{d\Omega} \approx \frac{\mu_0 q^2}{16\pi^3 c}\frac{(\Delta v)^2 \sin^2\psi}{\left(1-\bar{\beta}\cos\psi\right)^4}\frac{\sin^2 x}{x^2} \approx \frac{\mu_0 q^2 (\Delta v)^2}{\pi^3 c}\frac{\bar{\gamma}^6(\bar{\gamma}\psi)}{\left(1+(\bar{\gamma}\psi)^2\right)^4}\frac{\sin^2 x}{x^2},$$

where $x \equiv \frac{1}{2}\omega\Delta t\left(1-\bar{\beta}\cos\psi\right) \approx \frac{\omega\Delta t}{4\bar{\gamma}^2}\left(1+(\bar{\gamma}\psi)^2\right)$ and the highly relativistic/small angle

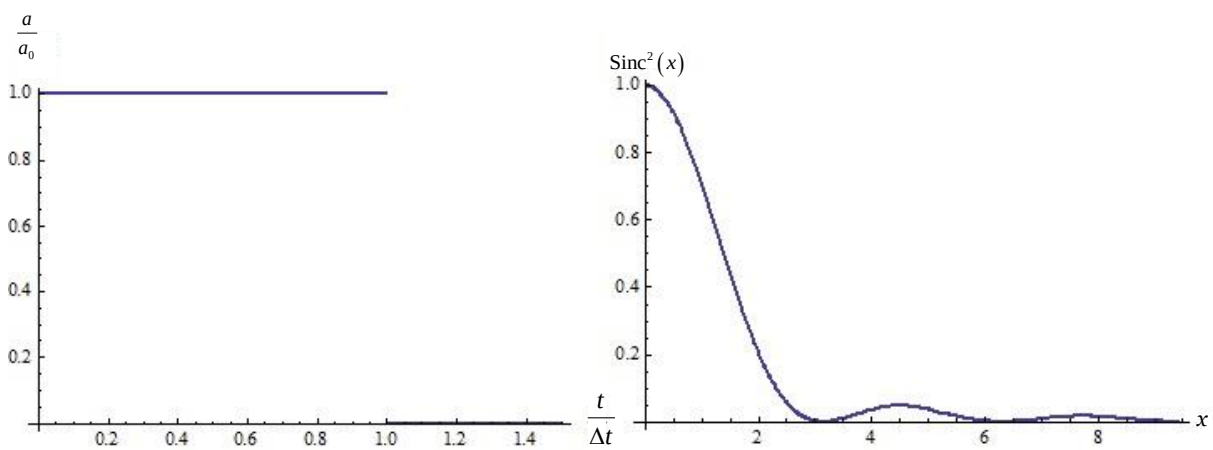

Figure 3: a) the normalized acceleration as a function of normalized time. b) the normalized frequency spectrum for a given constant angle.

approximation is made. The spectrum goes as sinc² and is related to the Fourier transform of the rect function in the acceleration. In the frequency domain, different angles from the axis are associated with different frequencies. The preponderance of radiation is emitted between

$0 \le x \le \pi$, so the cutoff frequency can be defined as $x_c = \pi$ and since x depends on angle then the cutoff frequency depends on angle

$$\omega_c = \frac{2\pi}{\Delta t\left(1-\bar{\beta}\cos\psi\right)} \approx \frac{4\pi\bar{\gamma}^2}{\Delta t\left(1+(\bar{\gamma}\psi)^2\right)}. \tag{4.5}$$

As the angle increases in (4.5) the cutoff frequency decreases, as shown in the figure, therefore higher frequencies are emitted close to the axis and lower frequencies are emitted everywhere. (4.5) is plotted in Figure 4 where the x-axis is $\bar{\gamma}\psi$ and the y-axis is $\omega_c\Delta t$. The highest intensity of radiation, found from Figure 3b, occurs at 0.5 on the x-axis and corresponds to a cutoff frequency of $\omega_c \approx \frac{16\pi\bar{\gamma}^2}{5\Delta t}$, or 80% of the peak value in Figure 4.

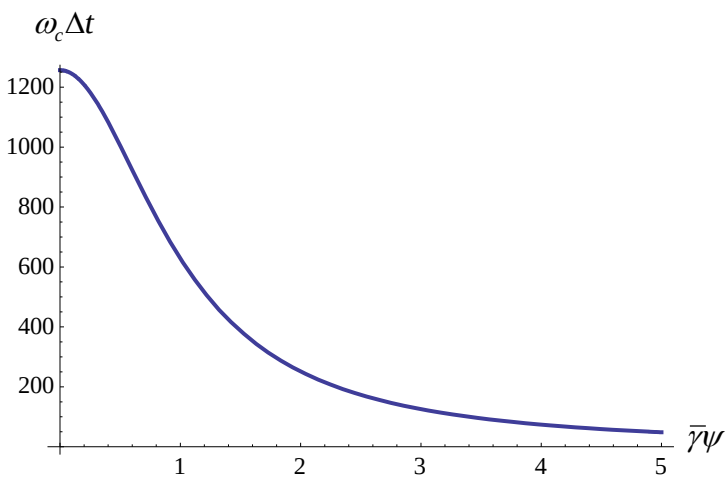

Figure 4: the angular dependence of the cutoff frequency.

There is no radiation directly on axis so that the peak cutoff frequency in Figure 4 is never attained.

Example 2: A linear acceleration burst for two particles

For two particles with an infinite accelerator the 2 particles would look like a single particle from infinitely far away so that the 2 particles would radiate like a single particle with twice the charge. In this case the two particles would split the radiated energy symmetrically such that they would execute the same motion and the starting distance between the two particles would always be the same.

Now add a second particle to the first example such that the second particle enters the accelerator after the first particle. For a second particle the form of the equation above will be the same but the variables will be slightly different

$$[R]_2 \approx 2\bar{\gamma}^2 \cos\theta_2 R_2,$$

where $R_2 \approx R_1\left(1+\frac{d}{R_1}\cos\theta_1\right)$ and $\cot\theta_2 = \cot\theta_1 + \frac{d}{R_1}\csc\theta_1$. Where d is the present distance between particle 1 and particle 2. It is assumed that $d \ll R_1$ and consequently be kept only to first order.

The angle θ_1 may be assumed to be small even though it is to be integrated over all values because the radiation will be primarily at small angles making contributions to the radiated energy at larger angles insignificant. The angle of the second particle can be approximated by looking at the power series of the cotangent and cosecant,

$$\theta_2 \approx \theta_1\left(1-\frac{d}{R_1}\right).$$

The retarded distance of the second particle is then

$$[R]_2 \approx 2\bar{\gamma}^2 \cos\left(\theta_1 - \frac{d}{R_1}\theta_1\right) R_1\left\{1+\frac{d}{R_1}\cos\theta_1\right\}.$$

Using a trig identity and keeping only terms first order in $\frac{d}{R_1}$ gives

$$[R]_2 \approx 2\bar{\gamma}^2 R_1\left\{\cos\theta_1 - \sin\theta_1 \sin\left(\frac{d}{R_1}\theta_1\right) + \frac{d}{R_1}\cos^2\theta_1\right\}.$$

The retarded times for the two particles are

$$
\begin{aligned}
t_{r1} &= t - \frac{2\bar{\gamma}^2 R_1}{c}\cos\theta_1 \\
t_{r2} &= t - \frac{2\bar{\gamma}^2 R_1}{c}\left\{\cos\theta_1 - \sin\theta_1 \sin\left(\frac{d}{R_1}\theta_1\right) + \frac{d}{R_1}\cos^2\theta_1\right\}
\end{aligned}
\tag{4.6}
$$

The assumptions that went into making (4.6) are that the particles have highly relativistic velocity and that the distance between the two particles is short compared to the distance to the imaginary surface at which the fields are to be evaluated. The assumption that the angle θ is small is a consequence of the highly relativistic assumption.

The retarded times (4.6) are in terms of the present time and present angle. We can shift the time to be coincident at the retarded time of the first particle and consequently call this the time t, in steps: $t_{r2} = t_{r1} + \frac{2\bar{\gamma}^2 R_1}{c}\left\{\sin\theta_1 \sin\left(\frac{d}{R_1}\theta_1\right) - \frac{d}{R_1}\cos^2\theta_1\right\}$, so calling $t_{r1} \equiv t$ allows the simplest expression of the retarded times

$$
\begin{aligned}
t_{r1} &= t \\
t_{r2} &= t + \frac{2\bar{\gamma}^2 R_1}{c}\left\{\sin\theta_1 \sin\left(\frac{d}{R_1}\theta_1\right) - \frac{d}{R_1}\cos^2\theta_1\right\}
\end{aligned}
\tag{4.7}
$$

The instantaneous radiated power for particle 1 is in terms of the retarded time for particle 1 which we are calling t. To look at the instantaneous radiated power of particle 1 it would be preferable to choose a surface centered on the retarded position of particle 1 and then integrate over the retarded angles associated with the retarded position of particle 1. Consequently, (4.7) should be expressed in terms of retarded distances and angles with respect to the 1st particle. A nearly identical analysis will result in

$$
\begin{aligned}
&[R_2] \approx [R_1]\left(1+\frac{[d]}{[R_1]}\cos\psi_1\right) \\
&\psi_2 \approx \psi_1\left(1-\frac{[d]}{[R_1]}\right) \\
&\phi_2 = \phi_1
\end{aligned}
\tag{4.8}
$$

and

$$
\begin{aligned}
&t_{r1} \equiv t \\
&t_{r2} \approx t - \frac{[d]}{c}\cos\psi_1 - \frac{[d]}{c}\sin\psi_1 \sin\left(\frac{[d]}{[R_1]}\psi_1\right).
\end{aligned}
\tag{4.9}
$$

Here the distance $[d]$ is the distance between the retarded positions of the 1st and 2nd particles. For the current arrangement with the focus on the 1st particle the distance is given by

$$
[d] = \frac{d}{1-\bar{\beta}\cos\psi_1} \approx 2\bar{\gamma}^2 d\ .
$$

The approximation is valid for small angles and large $\bar{\gamma}$. With the motion and the retarded times, the radiated Liénard-Wiechert electric field can be specified. The electric field is given by

$$
\vec{E} = \frac{q}{4\pi\varepsilon_0}\left[\frac{\hat{n}(\hat{n}\cdot\vec{\alpha})-\vec{\alpha}}{cRs^3}\right]
$$

where $[\hat{n}] = \cos\phi\sin\psi\hat{e}_x + \sin\phi\sin\psi\hat{e}_y + \cos\psi\hat{e}_z$, the normalized acceleration is $\vec{\alpha} \equiv \frac{\vec{a}}{c}$ and $s \equiv 1-\hat{n}\cdot\vec{\beta}$. So that for two particles

$$
\begin{aligned}
&\vec{E}_1 = \frac{q[\alpha_1]}{4\pi\varepsilon_0 c\left[R_1 s_1^3\right]}\left\{\sin\psi_1\cos\psi_1\left(\cos\phi_1\hat{e}_x + \sin\phi_1\hat{e}_y\right) - \sin^2\psi_1\hat{e}_z\right\} \\
&\vec{E}_2 = \frac{q[\alpha_2]}{4\pi\varepsilon_0 c\left[R_2 s_2^3\right]}\left\{\sin\psi_2\cos\psi_2\left(\cos\phi_2\hat{e}_x + \sin\phi_2\hat{e}_y\right) - \sin^2\psi_2\hat{e}_z\right\}
\end{aligned}
\tag{4.10}
$$

Including (4.8) with (4.10) and keeping only terms to first order in $\frac{[d]}{[R_1]}$,

$$\vec{E}_1 = \frac{q[\alpha_1]}{4\pi\varepsilon_0 c\left[R_1 s_1^3\right]}\left\{\sin\psi_1\cos\psi_1\left(\cos\phi_1\hat{e}_x + \sin\phi_1\hat{e}_y\right) - \sin^2\psi_1\hat{e}_z\right\}$$

(4.11)

$$\vec{E}_2 = \frac{q[\alpha_2]}{4\pi\varepsilon_0 c\left[R_1 s_2^3\right]}\left\{\begin{aligned}&\left(\sin\psi_1\cos\psi_1\cos\phi_1 + \frac{[d]}{[R_1]}\psi_1\sin^2\psi_1\cos\phi_1 - \frac{[d]}{[R_1]}\psi_1\cos^2\psi_1\cos\phi_1\right)\hat{e}_x \\ &+\left(\sin\psi_1\cos\psi_1\sin\phi_1 + \frac{[d]}{[R_1]}\psi_1\sin^2\psi_1\sin\phi_1 - \frac{[d]}{[R_1]}\psi_1\cos^2\psi_1\sin\phi_1\right)\hat{e}_y \\ &-\left(\sin^2\psi_1 - \frac{2[d]}{[R_1]}\psi_1\sin\psi_1\cos\psi_1\right)\hat{e}_z\end{aligned}\right\}.$$

Application of (3.6) and (4.11) provides two terms,

(4.12)
$$\vec{S}_1 = \frac{1}{\mu_0 c}\left[\hat{n}_1\right]\left\{\vec{E}_1^2 + \vec{E}_1\cdot\vec{E}_2\right\}$$

The first term in (4.12) would give the radiated power from the first particle if that particle were alone. The second term provides the correction to that radiated power due to interference effects: the different retarded times that appear in the accelerations and velocities results in some phase shift, as well as the spatial displacement of the two particles that is evident in the angular distribution of the fields. Putting (4.12) into (3.7) and integrating with Mathematica while making small angle approximations: $\sin\psi \approx \psi$ and $\cos\psi \approx \psi$ as well as limiting the integration over ψ_1 from 0 to $\frac{3}{\bar{\gamma}}$ gives

(4.13)
$$P_1(t) = \frac{81a^2q^2\left(\Theta(t) - \Theta(t-\Delta t)\right)\left(\bar{\gamma}^2 + 6\right)}{32\pi c^3\varepsilon_0\bar{\gamma}^6\left(1-\bar{\beta}\right)^5}\left\{1 + \left(1 - \frac{2[d]}{[R_1]}\right)\left(\Theta\left(t - \frac{[d]}{c}\right) - \Theta\left(t - \frac{[d]}{c} - \Delta t\right)\right)\right\}.$$

In order to judge the effectiveness of the approximations used, the power radiated from a single particle was found with Mathematica exactly and again with all of the approximations that were used in the calculation of (4.13). The result depends on γ, if $\gamma = 100$ the approximate result is 3755 times bigger than the exact result, if $\gamma = 200$ the approximate result is 3751.45 times bigger than the exact result, if $\gamma = 1000$ the approximate result is 3750.06 times bigger than the exact result, and if $\gamma = 5000$ the approximate result is 3750 times bigger than the exact result. This suggests that, to good approximation ($\sim 0.2\%$), for $\gamma > 100$ the power radiated by particle 1 in the presence of particle 2 is(4.13) divided by 3750. As $[R_1] \to \infty$ then (4.13) cleans up to

$$(4.14) \qquad P_1(t) = \frac{81a^2q^2}{3750\pi c^3\varepsilon_0}\bar{\gamma}^6\left\{\Theta(t) - \Theta(t-\Delta t)\right\}\left\{1 + \Theta\left(t - \frac{[d]}{c}\right) - \Theta\left(t - \frac{[d]}{c} - \Delta t\right)\right\}$$

The power in (4.13) goes roughly as $\bar{\gamma}^6$, as would be expected for bremsstrahlung radiation. The first term that appears in the curly brackets is due to the radiation of the first particle, and the particle would radiate approximately this much without the second particle present. The next term that contains a rect function, $\Theta\left(t - \frac{2\bar{\gamma}^2 d}{c}\right) - \Theta\left(t - \frac{2\bar{\gamma}^2 d}{c} - \Delta t\right)$, is additional radiation from the first particle due to the presence of the second particle (This additional radiation could, in principle, contribute negatively to the radiated power). The additional radiation consists of two terms; 1, which makes the radiation completely coherent, and $-\frac{4\bar{\gamma}^2 d}{R_1}$ which reduces the amount of coherence due to spatial displacement. In addition, if the two rect functions do not completely overlap, there can be reduced coherence as well. This is a result of the electric fields from the two particles not coinciding, emphasizing the interference

aspect of classical coherence. The electric field of both particles must exist at the same place and time for there to be interference and consequently what we call coherence.

The term coherence has many uses, for the purposes of this thesis, coherence is intended to describe the enhancement of spontaneous radiated power from classically coherent fields due entirely to interference. Classically the fields are coherent since the phase of the field at one point in space is completely determined by the phase of the field at a different point in space. If the two particles in this example were to radiate square waves that were back to back but not overlapping, then there would be a decrease in the bandwidth of the radiation, considered by some to be an increase in coherence, but it would still be considered incoherent radiation in this thesis since the power radiated would be the same as the two particles radiating independently. Coherence also has a statistical interpretation, consider a random initial phase space for multiple particles. Each individual initial phase space will predict a radiated power for the system, then an ensemble average of the radiated power for all of the possible initial phase spaces will yield a result for the radiated power that could be coherent, partially coherent, or incoherent.

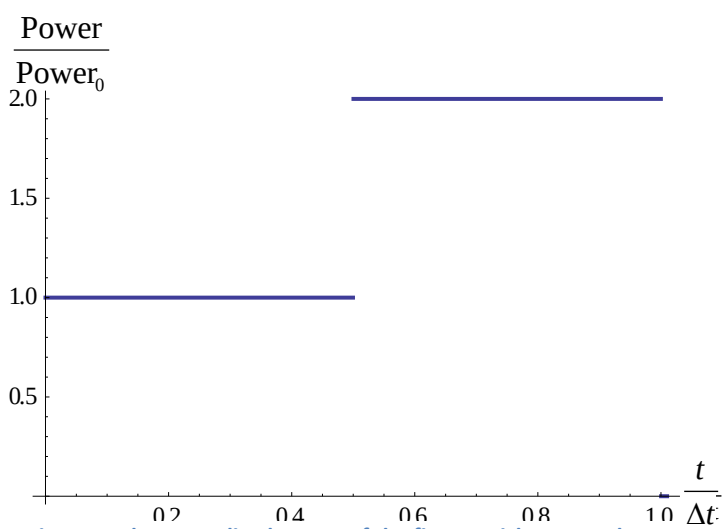

Figure 5: The normalized power of the first particle versus the normalized time. $\frac{[d]}{L} = 0.5$

The power radiated by the first particle is normalized by dividing out the power due to a single particle from (4.13) then plotted in Figure 5 versus the normalized time, $\frac{t}{\Delta t}$. The effects due to $\frac{[d]}{[R_1]}$ and $\frac{[d]}{c\Delta t}$ have been exaggerated in order to make them

apparent in the graph. When $d = 0$ the two pulses completely overlap and there is full coherence. As d increases the pulses no longer overlap completely and the enhancement of the parts that do overlap is decreased, as the interference is increasingly dephased. When the pulses no longer overlap the radiation is completely incoherent. By defining the length of acceleration as $L \equiv \bar{\beta} c \Delta t \approx c \Delta t$, the distance between the particles is defined with respect to the length of acceleration.

To find the power radiated by the second particle, the retarded time and distance must be found again, because they will be dramatically different for highly relativistic particles. The particles will not, in principle, radiate symmetric amounts of energy, one could radiate more than another. However, all of the main features that are present in the radiated power of the first particle (overlapping electric fields, coherence due to interference, and dephasing as the present distance between the particles is increased) will be present in the second particle's radiated power. In addition, once the power is found they cannot be added to find the total power radiated by both particles because the powers found are the instantaneous powers that occur at the time of emission. The emission times for the two particles are not simultaneous. This could be avoided by defining time with respect to the 1st particles retarded time, i.e. choose the same zero of time. The retarded time will be different primarily because the retarded distances are so different, in particular,

$$[d] = \frac{d}{1 + \bar{\beta} \cos \psi_2} \approx \frac{d}{2}.$$

The surface now under investigation is to be centered around the 2nd particle and the time is to be retarded to the 2nd particle. The angles are now

$$
\begin{aligned}
&[R_1] \approx [R_2]\left(1-\frac{[d]}{[R_2]}\cos\psi_2\right) \\
&\psi_1 \approx \psi_2\left(1+\frac{[d]}{[R_2]}\right) \\
&\phi_1 = \phi_2
\end{aligned}
\tag{4.15}
$$

And the retarded times are

$$
\begin{aligned}
&t_{r2} \equiv t \\
&t_{r1} \approx t + \frac{[d]}{c}\cos\psi_2 + \frac{[d]}{c}\sin\psi_2 \sin\left(\frac{[d]}{[R_2]}\psi_2\right)
\end{aligned}
\tag{4.16}
$$

In (4.16) we can see that the retarded time for particle 1 is ahead of the retarded time for the 2nd particle, at least in the forward direction. The electric fields are then, with (4.15),

(4.17)

$$
\vec{E}_2 = \frac{q[\alpha_2]}{4\pi\varepsilon_0 c\left[R_2 s_2^3\right]}\left\{\sin\psi_2\cos\psi_2\left(\cos\phi_2\hat{e}_x + \sin\phi_2\hat{e}_y\right) - \sin^2\psi_2\hat{e}_z\right\}
$$

$$
\vec{E}_1 = \frac{q[\alpha_1]}{4\pi\varepsilon_0 c\left[R_2 s_1^3\right]}\left\{\begin{aligned}
&\left(\sin\psi_2\cos\psi_2\cos\phi_2 - \frac{[d]}{[R_2]}\psi_2\sin^2\psi_2\cos\phi_2 + \frac{[d]}{[R_2]}\psi_2\cos^2\psi_2\cos\phi_2\right)\hat{e}_x \\
&+\left(\sin\psi_2\cos\psi_2\sin\phi_2 - \frac{[d]}{[R_2]}\psi_2\sin^2\psi_2\sin\phi_2 + \frac{[d]}{[R_2]}\psi_2\cos^2\psi_2\sin\phi_2\right)\hat{e}_y \\
&-\left(\sin^2\psi_2 + \frac{2[d]}{[R_2]}\psi_2\sin\psi_2\cos\psi_2\right)\hat{e}_z
\end{aligned}\right\}.
$$

This time the integral to find the power is over the 2nd particles retarded angles. The power for the 2nd particle is

$$
P_2(t) = \frac{81a^2q^2\left(\Theta(t)-\Theta(t-\Delta t)\right)\left(\bar{\gamma}^2+6\right)}{32\pi c^3\varepsilon_0\bar{\gamma}^6\left(1-\bar{\beta}\right)^5}\left\{1+\left(1+\frac{2[d]}{[R_2]}\right)\left(\Theta\left(t+\frac{[d]}{c}\right)-\Theta\left(t+\frac{[d]}{c}-\Delta t\right)\right)\right\}
\tag{4.18}
$$

, which is very similar to (4.13) except that $[d]$ is different. In order to compare these results,

Mathematica was used to integrate (4.13) and (4.18) for the duration of the acceleration, Δt. The time duration is Δt because the times are shifted not Lorentz transformed. The energy radiated, in total, for the particles during the acceleration burst is

$$
\begin{aligned}
U_1 &= P_0\left\{\Delta t+\Theta\left(\Delta t-\frac{2\bar{\gamma}^2 d}{c}\right)\left(1-\frac{4\bar{\gamma}^2 d}{[R_1]}\right)\left(\Delta t-\frac{2\bar{\gamma}^2 d}{c}\right)\right\} \\
U_2 &= P_0\left\{\Delta t+\Theta\left(\Delta t-\frac{d}{2c}\right)\left(1+\frac{d}{[R_2]}\right)\left(\Delta t-\frac{d}{2c}\right)\right\}
\end{aligned}
\tag{4.19}
$$

where $P_0=\dfrac{81a^2q^2\left(\bar{\gamma}^2+6\right)}{32\pi c^3\varepsilon_0\bar{\gamma}^6\left(1-\bar{\beta}\right)^5(3750)}$. Except in the case of very small $\dfrac{d}{c}$ the 1st particle will radiate as though it is alone because the step function will kill the interference term. The 2nd particle will see most of the enhancement in radiated energy because $\dfrac{d}{c}$ can become larger before the radiated energy is reduced to the single particle case.

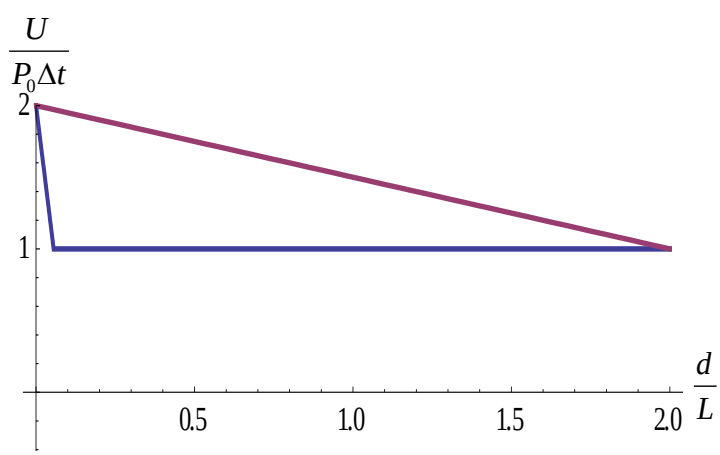

Figure 6: The normalized energy radiated by the two particles; the blue line represents the 1st particle and the red line represents the 2nd particle, $\bar{\gamma}=3$ and $R\to\infty$.

In Figure 6, the total normalized radiated energy is drawn for both particles with the present distance varying from 0 to $3L$. As the distance is increased the red line (energy of the 2nd particle) decreases linearly until it reaches 1 at $\dfrac{d}{L}=2$. When the present distance is reduced to 0 the blue line will increase up to 2. The blue line

(energy of the 1st particle) will do the same except that there is a factor of $4\bar{\gamma}^2$ that augments the present distance and prevents the radiation of excess energy for any but the smallest values of d. As a consequence it is the 2nd particle that enters the accelerator that demonstrates the most change in radiated energy. This energy dependence indicates that the point charge will radiate coherently if the retarded position of the other point charge is in the accelerator at the same time as the point charge of interest.

The radiated spectrum for both particles is found from an extension of (4.4).

$$\frac{dI(\omega)}{d\Omega} \approx \frac{\mu_0 q^2}{16\pi^3 c}\left|\frac{\hat{n}\times\Delta\vec{v}}{\left(1-\hat{n}\cdot\vec{\bar{\beta}}\right)^2\Delta t}\right|^2 \left|\int_0^{\Delta t} e^{i\omega\left(1-\hat{n}\cdot\vec{\bar{\beta}}\right)\tau} d\tau + \int_0^{\Delta t} e^{i\omega\left(1-\hat{n}\cdot\vec{\bar{\beta}}\right)\left(\tau-\frac{d}{\bar{\beta}c}\right)} d\tau\right|^2, \tag{4.20}$$

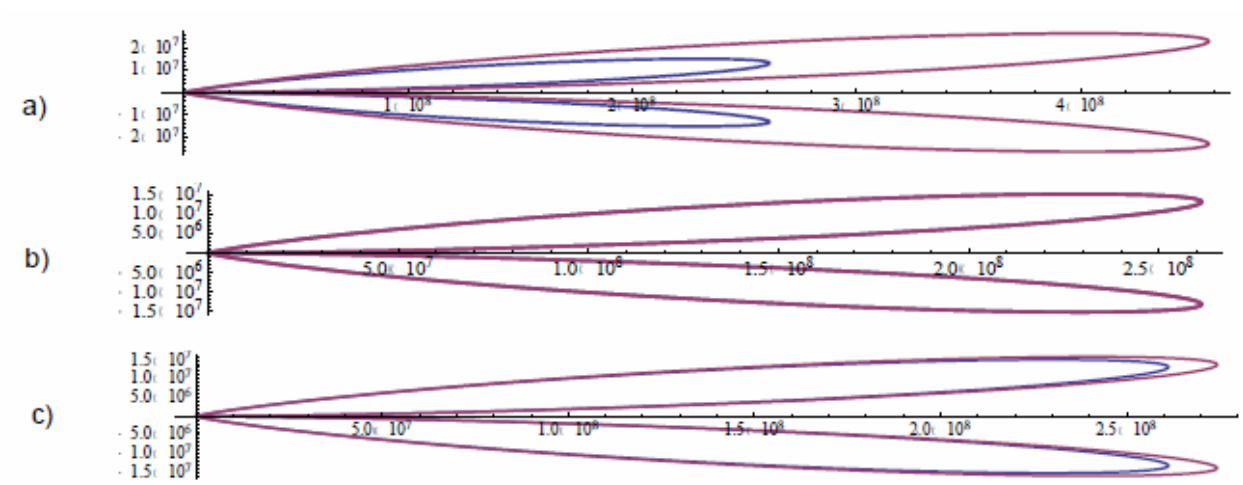

Figure 7: The angular distribution of the radiated energy of a single particle with a second particle present in red, for comparison a single particle alone is in blue; a) has the present distance equal to one quarter of the length of acceleration, b) has a present distance that is one and a quarter times the length of acceleration, and c) has a present distance that is 95% of the acceleration length.

after integrating (4.20) the complex exponentials can be reduced to trigonometric functions so that the total radiated spectrum for the system is

(4.21) $$\frac{dI(\omega)}{d\Omega}_{\text{System}} = 4\cos^2\left(\frac{d}{L}x\right)\frac{dI(\omega)}{d\Omega}_{\text{Single}},$$

where $\frac{dI(\omega)}{d\Omega}_{\text{Single}}$ is the radiated spectrum of a single particle found from (4.4). (4.21) is integrated over ω and plotted in Figure 7. A comparison with the single particle alone case shows that the angular distribution of energy grows in the presence of a second particle but is distributed with the same angular spread. However, the frequency spectrum has a much narrower bandwidth as shown in Figure 8. In Figure 8 the main part of the spectrum of the two particles reaches 0 before 2 and then remains close to zero until around 3.4. While the spectrum of a single particle has the first zero occur at 3.14. The peaks in the two plots occur in roughly the same place but the troughs for the two particle case occur earlier and last longer making two separated frequency bands. Interference will only occur if the retarded positions of both electrons are such that they both occur in the accelerator.

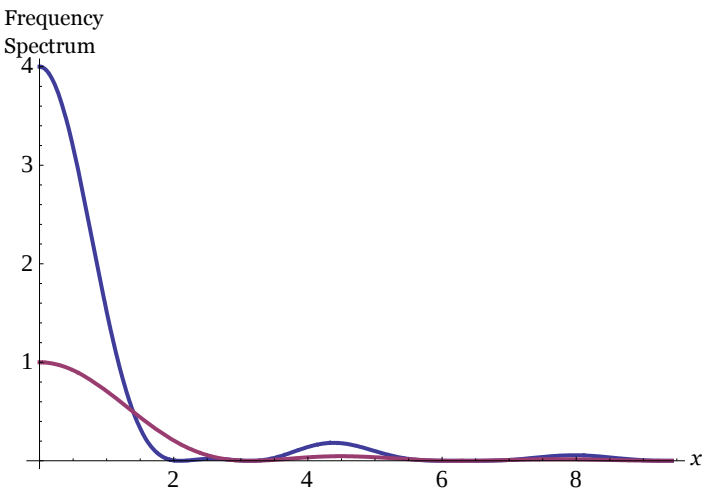

Figure 8: In blue, the frequency spectrum of 2 particles with a present distance that is three quarters of the acceleration length. In red, the frequency spectrum of a single particle.

From the Kimel-Elias formula for power loss due to radiation [4],

(4.22) $$\left[\frac{d\gamma_1(t)}{dt}\right] = -\frac{2r_e\bar{\gamma}^4}{3c}\left\{\bar{\gamma}^2\alpha_1^2(t) + \left[\bar{\gamma}^2\alpha_1(t)\alpha_2(t_{r2})\right]\right\}.$$

There is one issue that must be resolved in (4.22); what is the retarded time t_{r2}? The retarded time is supposed to be the retarded time of the 2nd particle with respect to the imaginary surface

only rescaled by the retarded time of the 1st particle with respect to the same imaginary surface. This is complicated by the observation that a surface that is equidistant from the retarded position of the 1st particle does not have surface elements that are equidistant to the retarded position of the 2nd particle. As the surface is integrated over, the retarded time of the 2nd particle will vary. However, for highly relativistic particles the radiation is strongly directional making one retarded time (as well as one portion of the imaginary surface) much more important than the others. For the case of linear motion the radiation will be directed strongly along the velocity axis. As a result, the retarded time in (4.22) must be related to a distance along this axis and comparison to (4.13) suggests that

$$t_{r2} = t - \frac{[d]}{c}.$$

This is the retarded time between the particles.

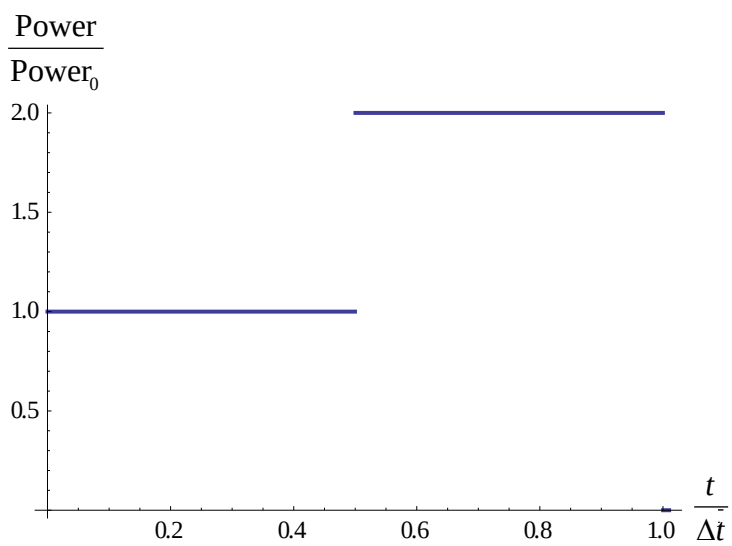

Figure 9: The normalized power radiated by particle 1 as a function of the normalized time.

Figure 9 shows the normalized power radiated by particle 1 versus the normalized time and should be compared to Figure 5. Figure 9 looks the same as Figure 5. The power radiated in (4.22) shows no dephasing as the particles are separated. This is due to the zeroeth order approximation for the angles that was used in [4].

[4] assumes that the principle cause of coherence is the phase change due to the retarded times and ignores the small phase changes due to the change in retarded angles. Associated with the change in retarded angles is a small change in the direction of the electric field which also effects magnitude of the interference term. The spatial dephasing is ignored because the distance to the imaginary surface is considered to be so large that the temporal dephasing will dominate. This is largely borne out, as shown by Figure 5 where the dominant effect is the overlap of the electric fields that is driven by the retarded times, while the change in amplitude of the interference due to the retarded angles is so small it cannot be seen.

The non-causal version of the Kimel-Elias equation shows the same results as (4.13) and (4.18) except the possibility of having a different retarded angle was not included in [4]. In this case the retarded times are given by

$$t_{r2} = t - \frac{2\bar{\gamma}^2 d}{c} \quad t_{r1} = t + \frac{d}{2c}.$$

The time t that appears in the retarded times above is not the same time due to using $\vec{\alpha} = \vec{\alpha}_0 \left[\Theta(t) - \Theta(t - \Delta t) \right]$ for both 1 and 2. In order to compare the results of the Kimel-Elias power equations the time must be integrated to find the energy radiated, which is comparable.

Alternatively the time can be shifted to make them the same times. When the power radiated by particle 1 is considered, the zero of time is taken to be when the 1st particle enters the accelerator. When the power radiated by the 2nd particle is considered, the zero of that time is taken to be when the 2nd particle enters the accelerator. The difference between the two times is a constant which can be incorporated at the end. For the power radiated by the 2nd particle,

subtract the time it takes for the 2nd particle to reach the accelerator when the 1st particle has just reached the accelerator, $\frac{d}{c}$. Now the times for the powers are the same.

In conclusion, the point charges in an infinite linear accelerator will always interfere constructively. When the accelerator is finite the retarded positions of both point charges must be in the accelerator in order to get constructive interference. If the retarded positions of the point charges are not in the accelerator together, there will not be interference of the radiated fields at a very distant surface and they will radiate as if they are alone. The two point charges do not have symmetry in their retarded positions so that one can radiate more than the other if the interference condition is satisfied for one and not the other.

Example 3: Synchrotron Radiation

Synchrotron radiation involves relativistic point charges undergoing circular motion. The radiation is still very directional and is reminiscent of a lighthouse. As seen in the last example, the coherent effects are based in interference. For linear motion the radiation from the two particles had very similar angular distributions so that the fields overlapped on a distant surface. For circular motion, small displacements in distance can radically alter the angular distribution of radiation on a distant surface. Consequently synchrotron radiation is not a good candidate for the Kimel-Elias equation. The retarded time would not be the determinative factor that decided if there was coherent radiation or not. Instead the angular distribution of radiation, essentially $\psi \sim \frac{1}{\gamma}$, would determine how close together the retarded positions of the particles would have to be in order to radiate coherently, $[d] < R/\gamma$ where R is the radius of the circular motion.

Example 4: Free Electron Laser

For a Free Electron Laser (FEL) the spontaneous radiation is usually overwhelmed by the stimulated emission. An exception can occur in Self-Amplified Spontaneous Emission (SASE) that takes place in undulators that do not have a resonator when the charges are spaced such that $\vec{E} \cdot \vec{J}$ is very small. The Stanford Linear Accelerator has been turned into just such a light source for X-rays. There are existing simulations of particle motion and field amplitude evolution that work in the small gain regime or in the saturated regime for stimulated emission but none that I know of that include spontaneous emission. The directed and overlapping nature of the radiation that is emitted by an electron in an undulator make this a good candidate for the Kimel-Elias approach. By including the radiation reaction, a simulation of the particle phase spaces and field amplitudes can be predicted for SASE FELs with specific spacing of the charges as well as the start-up of FELs with resonators.

The amplitude of the transverse motion of the particle depends on the inverse of the momentum of the particle, so a highly relativistic particle will have very little transverse motion and could be approximated by linear motion. The main difference between the FEL and the acceleration burst in example 2 is the acceleration of the particles. The retarded distances and times will be essentially the same, while the different accelerations will cause the radiated fields to be different and ultimately the radiated power to be different.

The FEL is characterized by the undulator parameter

$$K \equiv \frac{eB}{mc^2 k_u},$$

in Gaussian units. [11] The undulator magnets switch polarity with a wavelength of $\lambda_u = \frac{2\pi}{k_u}$.

The normalized velocity of the electrons passing through the undulator is given by

$$\vec{\beta} = -\frac{K}{\gamma}\cos\left(k_u z\right)\hat{e}_x + \left(\bar{\beta}_z - \frac{K^2}{4\gamma^2}\cos\left(2k_u z\right)\right)\hat{e}_z ,$$

with $\bar{\beta}_z \equiv 1 - \frac{1 + K^2/2}{2\gamma^2}$. [11] If the undulator parameter is much smaller than 1 and γ is much larger than 1, then the velocity is essentially the speed of light in the z- direction. At the same time the normalized acceleration is dominated by

(4.23) $$\alpha_x = \frac{Kk_u c}{\gamma}\sin\left(k_u z\right).$$

The acceleration in the z-direction goes as the undulator parameter squared and can be ignored. The motion of an electron passing through the undulator is then one dimensional in the z-direction despite having transverse acceleration. The wavelength of the emitted light is then $\lambda = \frac{\lambda_u}{2\bar{\gamma}^2}$. [11]

With this information the non-causal version of the Kimel-Elias equations can be invoked. The acceleration of the two particles under consideration, particle 1 entering the undulator before particle 2, can be found with reference to (4.23) where the 2nd particle will enter the undulator after an additional distance d. In this instance, an infinite undulator will be considered and the discussion of which particle enters the undulator first is an aid to determining the phase shift of the particles with respect to each other. The acceleration is

(4.24)
$$\alpha_{x1} = \frac{Kk_u c}{\bar{\gamma}} \sin\left(k_u z(t)\right)$$
$$\alpha_{x2} = \frac{Kk_u c}{\bar{\gamma}} \sin\left(k_u z(t) - k_u d\right),$$

Where $z(t) = \bar{\beta}_z ct$ is the position of the 1st particle along the beam axis. The second particle, at the same time, is behind the 1st particle by a distance d. To first find the energy loss of the 1st electron the retarded time of the 2nd electron is required. It was found earlier to be $t_{r2} = t - \frac{2\bar{\gamma}^2 d}{c}$. Then the Kimel-Elias equation for electron 1 is [4]

(4.25)
$$\frac{d\gamma_1}{dt} = -\frac{2r_e\bar{\gamma}^4}{3c}\left\{\alpha_{x1}{}^2(t) + \alpha_{x1}(t)\alpha_{x2}(t_{r2})\right\}.$$

With (4.24) and the retarded time, the engery loss given by (4.25) is

(4.26)
$$\frac{d\gamma_1}{dt} = -A\left\{\sin^2(\phi) + \sin(\phi)\sin\left(\phi - \left(2\bar{\gamma}^2 + 1\right)\psi\right)\right\},$$

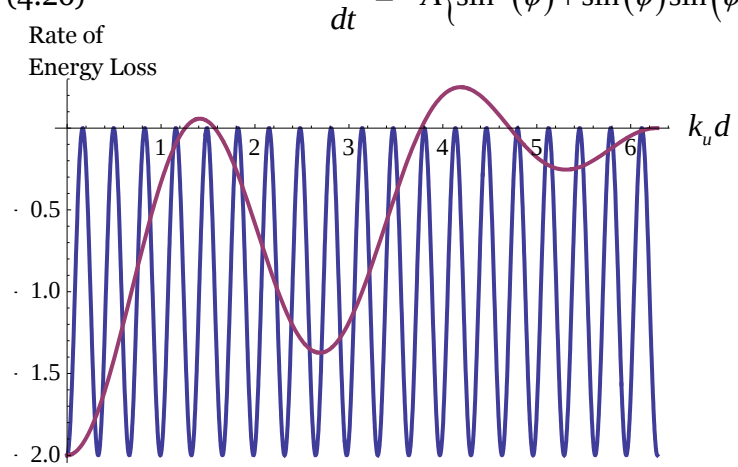

Figure 10: The normalized rate of energy loss versus normalized distance is plotted in blue for the 1st particle and in red for the 2nd particle. $\bar{\gamma} = 3$

where $\phi \equiv k_u z$, $\psi \equiv k_u d$ and $A \equiv \frac{2r_e K^2 k_u{}^2 \bar{\gamma}^2 c}{3}$. Also r_e is the classical electron radius.

The energy loss for the 2nd particle is found from (4.24) the Kimel-Elias equation and the retarded time for the first particle, $t_{r1} = t + \frac{d}{2c}$,

(4.27) $$\frac{d\gamma_2}{dt} = -A\left\{\sin^2(\phi-\psi)+\sin(\phi-\psi)\sin\left(\phi-\frac{3}{2}\psi\right)\right\},$$

with all of the definitions the same as for the first case. (4.26) and (4.27) are plotted in Figure 10. The present distance between the electrons is varied over one undulator period in the plot. The 1st electron is ahead of the 2nd electron and experiences a rapid oscillation between zero and -2, shown in blue. $\bar{\gamma}=3$ was chosen in order to prevent the number of oscillations from becoming too large on the plot. The 2nd electron has a more interesting and slowly varying plot in red. At two locations on the plot the 2nd electron gains energy rather than losing energy. Also, the plot of the 2nd electron is periodic with a period of two undulator periods.

By integrating over time for one period of the undulator, the energy change per undulator period can be found,

(4.28) $$\begin{aligned}\frac{\Delta U_1}{\text{period}} &= -\frac{Amc\pi}{k_u}\left\{1+\cos\left(\psi+2\bar{\gamma}^2\psi\right)\right\}\\ \frac{\Delta U_2}{\text{period}} &= -\frac{Amc\pi}{k_u}\left\{2\cos^2\left(\frac{\psi}{4}\right)\right\}\end{aligned}.$$

This is the energy lost by the electrons per undulator period. The energy radiated per undulator

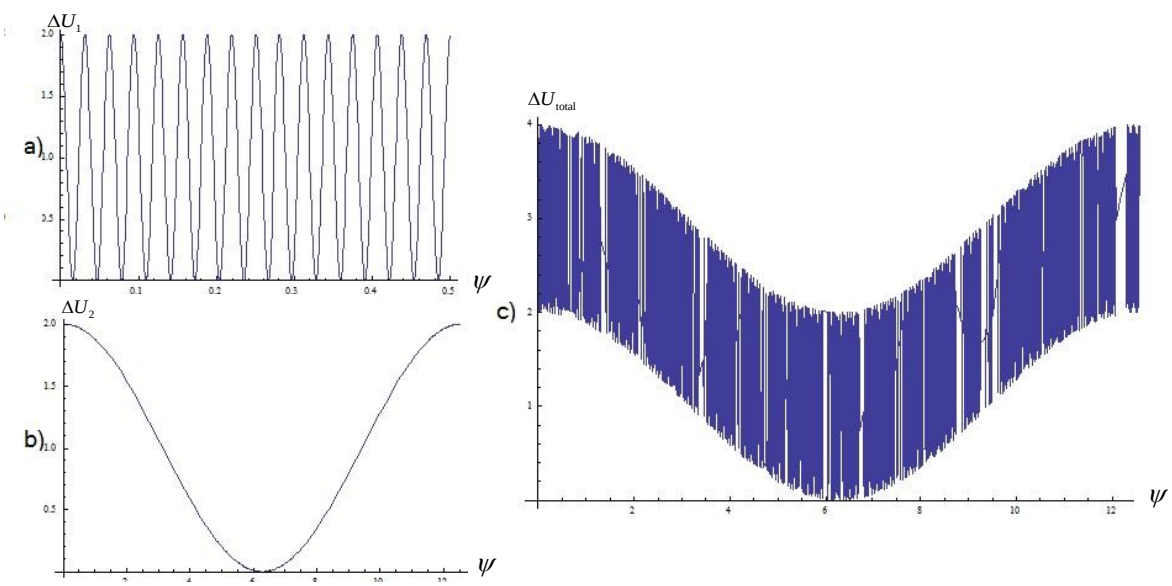

Figure 11: The energy radiated per period as a function of the distance between the particles for a) the first electron, b) the second electron and c) both electrons together. In part c) the gaps are artifacts of the plotting program.

period is the opposite of (4.28) and is plotted as a function of the distance between the electrons in Figure 11 parts a) and b). The plot in Figure 11 combines the energy radiated per undulator period of both electrons and gives the total energy radiated per undulator period. From Figure 11, as the distance between the particles is increased the radiation sees total coherence periodically with a period of 2 undulator periods. In addition no energy is radiated at a distance of one undulator period spacing. This says that two electrons in an infinite undulator ($K \ll 1$) will radiate maximally if they are spaced with even multiples of the undulator wavelength, and there will be no radiation at all if they are spaced with odd multiples of the undulator wavelength. However, if γ is large then the maximal and minimal radiation zones will be very unstable as small shifts in the distance will cause large variations in the total energy radiated. This is principally caused by the rapid oscillations in the radiation of the 1st electron. Making the undulator finite would cause many of the effects that were found in Example 2 and prevent the total energy radiated from being completely periodic as a function of the distance between the electrons. The distance scale that determines the energy loss for the 2nd electron is the undulator wavelength. The energy loss is periodic with period $2\lambda_u$. For the 1st electron, the distance scale that determines the energy loss is the radiated wavelength, λ. The energy loss is periodic with period λ. Figure 12

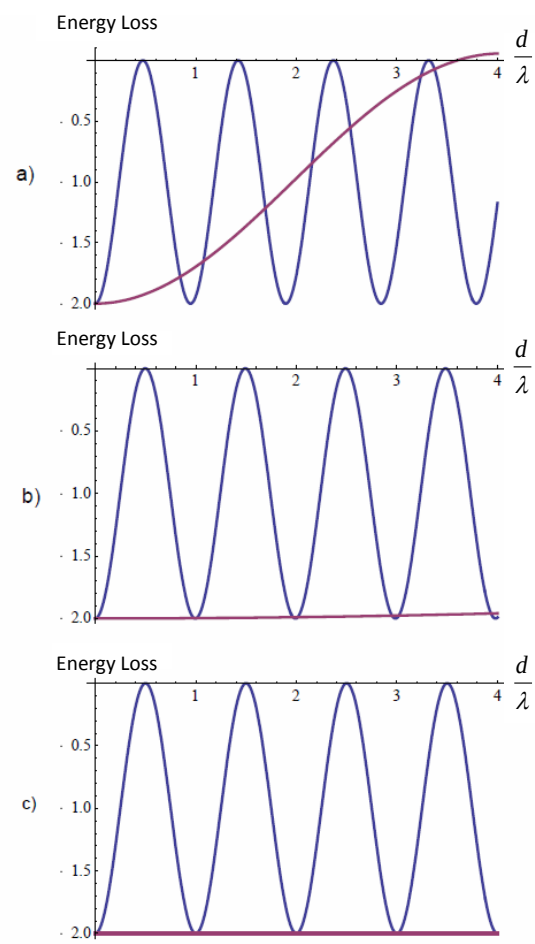

Figure 12: The Energy loss of both electrons as a function of distance divided by the radiated wavelength. a) $\bar{\gamma} = 3$ b) $\bar{\gamma} = 10$ c) $\bar{\gamma} = 100$

shows the energy loss just as Figure 10 except the scale has been changed so that the present distance between the electrons is in terms of the radiated wavelength. Also, the energy is changed so that $\bar{\gamma}$ is 3 in Figure 12 a), 10 in b) and 100 in c). The interference that the 1st electron sees scales with $\bar{\gamma}$ such that the energy loss is maximum at distances that are multiples of the radiated wavelength.

In conclusion, the point charges in an infinite undulator will radiate power that can exhibit constructive or destructive interference depending on the relative phase of the radiated electric and magnetic fields from the point charges. The relative phase difference is governed by the retarded distances. The retarded distances now depend on the present distance, the undulator period and the energy of the point charges. Again the two point charges are not symmetric in their retarded distances. This is responsible for the possibility of very different amounts of radiated energy from the two point charges.

Conclusions

The Kimel-Elias approach is applicable in instances where the particles are highly relativistic, and the radiation of the particles is very directional and overlapping nearly completely. In these cases the interference is dominated by the retarded distance between the particles which can be found by choosing the point on the imaginary surface as being the point where there is maximal and highly directed radiation. With these conditions satisfied the application of the Kimel-Elias equation is straight forward and relatively easy to implement.

The introduction of a second point charge has muddled the concept of causality. The interference that takes place at the field point far away from the sources defines the amount of radiation that each point charge radiates. However, due to the separation of the point charges, one of the charges is, in general, closer to the field point than the other point charge and will

radiate at a later time than the further away point charge. This leads to the idea that the completely retarded, and thus causal, fields of the point charge that is farther away from the field point are dependent on what the fields of the closer point charge will be at a later time. The mechanism that is responsible for making the retarded fields dependent on future conditions is the ad hoc imposition of energy conservation.

Chapter 5. Two Non-relativistic Dipole Radiators

The same procedure can be followed in the non-relativistic case. Consider two point charges, both with charge q, situated a distance d from each other. The charges are then induced to oscillate by mechanical means at a fixed frequency ω. The amplitude of oscillation is b, as shown in Figure 13. The particles are located on an axis which is in the same direction as their motion. The motion of the two point charges is given by

$$\begin{aligned} \vec{x}_1 &= -\frac{d}{2}\hat{e}_z + b\cos\left(\omega t + \frac{\phi}{2}\right)\hat{e}_z \\ \vec{x}_2 &= \frac{d}{2}\hat{e}_z + b\cos\left(\omega t - \frac{\phi}{2}\right)\hat{e}_z \end{aligned} \quad (5.1)$$

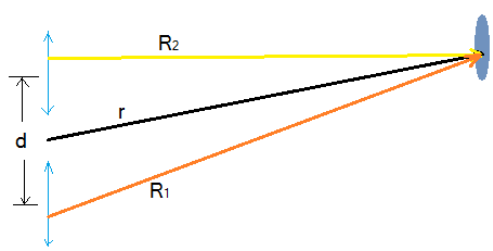

Figure 13: Two point charges that oscillate with constant frequency a distance d apart.

The phase ϕ is the relative phase between the two point charges and has been distributed symmetrically between the two particles. The normalized velocity is then

$$\begin{aligned} \vec{\beta}_1 &= \frac{1}{c}\frac{d\vec{x}_1}{dt} = -\frac{b\omega}{c}\sin\left(\omega t + \frac{\phi}{2}\right)\hat{e}_z \\ \vec{\beta}_2 &= \frac{1}{c}\frac{d\vec{x}_2}{dt} = -\frac{b\omega}{c}\sin\left(\omega t - \frac{\phi}{2}\right)\hat{e}_z \end{aligned} \quad (5.2)$$

Since this is to be non-relativistic, $\frac{b\omega}{c} \ll 1$. The normalized, although not dimensionless, acceleration is given by

$$\vec{\alpha}_1 = \frac{d\vec{\beta}_1}{dt} = -\frac{b\omega^2}{c}\cos\left(\omega t + \frac{\phi}{2}\right)\hat{e}_z$$
$$\vec{\alpha}_2 = \frac{d\vec{\beta}_2}{dt} = -\frac{b\omega^2}{c}\cos\left(\omega t - \frac{\phi}{2}\right)\hat{e}_z \quad . \tag{5.3}$$

The motion has now been sufficiently described to find the electric field.

The non-relativistic version of the Liénard-Wiechert radiation field is

$$\vec{E} = \frac{q}{4\pi\varepsilon_0 c}\left[\frac{\hat{n}\times\left(\hat{n}\times\hat{\alpha}\right)}{R}\right]_{\text{ret}}$$

where the far-field approximation was used and also the field is still retarded. The retardation condition imposed by the finite velocity of light is not a relativistic effect. The distance R is the distance from the source's retarded position to the point of observation. It should be clear from [Figure] that $\left[\vec{R}_1\right] = \vec{r} - \left[\vec{x}_1\right]$ and $\left[\vec{R}_2\right] = \vec{r} - \left[\vec{x}_2\right]$, the magnitudes are then given by

$$\left[R_1\right] = \sqrt{r^2 + \left[x_1\right]^2 - 2\vec{r}\cdot\left[\vec{x}_1\right]} \approx r - \hat{e}_r \cdot \left[\vec{x}_1\right]$$
$$\left[R_2\right] = \sqrt{r^2 + \left[x_2\right]^2 - 2\vec{r}\cdot\left[\vec{x}_2\right]} \approx r - \hat{e}_r \cdot \left[\vec{x}_2\right] \quad .$$

The far field approximation was used again where terms up to zeroeth order in r were kept. Now the time it takes for light to go from the retarded position of the source to the point of observation on the surface can be found. The retarded time is found from

$$t_{r1} = t - \frac{\left[R_1\left(t_{r1}\right)\right]}{c} \approx t - \frac{r}{c} + \frac{\hat{e}_r \cdot \left[\vec{x}_1\left(t_{r1}\right)\right]}{c}$$
$$t_{r2} = t - \frac{\left[R_2\left(t_{r2}\right)\right]}{c} \approx t - \frac{r}{c} + \frac{\hat{e}_r \cdot \left[\vec{x}_2\left(t_{r2}\right)\right]}{c}$$

The retarded times are transcendental equations which can be solved numerically, analytically in special cases, or by approximation. From (3.3), the Poynting vectors for the two particles separately are

$$\begin{aligned} \vec{S}_1 &= \frac{1}{\mu_0 c}\left\{\hat{n}_1\left|\vec{E}_1\right|^2 + \left(\hat{n}_2\left(\vec{E}_1\cdot\vec{E}_2\right) - \vec{E}_2\left(\hat{n}_2\cdot\vec{E}_1\right)\right)\right\} \\ \vec{S}_2 &= \frac{1}{\mu_0 c}\left\{\hat{n}_2\left|\vec{E}_2\right|^2 + \left(\hat{n}_1\left(\vec{E}_1\cdot\vec{E}_2\right) - \vec{E}_1\left(\hat{n}_1\cdot\vec{E}_2\right)\right)\right\} \end{aligned} . \tag{5.4}$$

The first term in each gives the amount of power that would be radiated if the two particles were alone. The term in () is due to the presence of the other particle and is the cross product of the electric field of the primary particle with the magnetic field of the other particle. Another way to express (5.4) is

$$\begin{aligned} \vec{S}_1 &= \frac{1}{\mu_0}\vec{E}_1\times\left(\vec{B}_1+\vec{B}_2\right) \\ \vec{S}_2 &= \frac{1}{\mu_0}\vec{E}_2\times\left(\vec{B}_1+\vec{B}_2\right) \end{aligned} .$$

The coherence effect that can lead to N^2 power is evidently due to the superposition of the magnetic fields for this choice of the partial Poynting vector $\vec{S}_j$. An alternate choice of the partial Poynting vector could suggest other sources for the coherence effect while not affecting the final result for energy loss from each particle.

To find the power each particle radiates separately, the following approximate results are needed:

$$\hat{n}_1 = \frac{\vec{R}_1}{R} \approx \frac{\vec{r}-\vec{x}_1}{r}\left(1+\frac{\hat{e}_r\cdot\vec{x}_1}{r}\right) \approx \hat{e}_r\left(1+\frac{\hat{e}_r\cdot\vec{x}_1}{r}\right)-\frac{\vec{x}_1}{r}$$

$$\hat{n}_2 = \frac{\vec{R}_2}{R} \approx \frac{\vec{r}-\vec{x}_2}{r}\left(1+\frac{\hat{e}_r\cdot\vec{x}_2}{r}\right) \approx \hat{e}_r\left(1+\frac{\hat{e}_r\cdot\vec{x}_2}{r}\right)-\frac{\vec{x}_2}{r}$$

(5.5) $$\hat{n}_1\cdot\hat{n} = \hat{n}_1\cdot\hat{e}_r \approx 1+\frac{\hat{e}_r\cdot\vec{x}_1}{r}-\frac{\hat{e}_r\cdot\vec{x}_1}{r} \approx 1$$.

$$\hat{n}_2\cdot\hat{n} = \hat{n}_2\cdot\hat{e}_r \approx 1+\frac{\hat{e}_r\cdot\vec{x}_2}{r}-\frac{\hat{e}_r\cdot\vec{x}_2}{r} \approx 1$$

$$\hat{n}_1\cdot\hat{n}_2 \approx \left(\hat{e}_r\left(1+\frac{\hat{e}_r\cdot\vec{x}_1}{r}\right)-\frac{\vec{x}_1}{r}\right)\cdot\left(\hat{e}_r\left(1+\frac{\hat{e}_r\cdot\vec{x}_2}{r}\right)-\frac{\vec{x}_2}{r}\right) \approx 1+\frac{\hat{e}_r\cdot\vec{x}_1}{r}+\frac{\hat{e}_r\cdot\vec{x}_2}{r}-\frac{\hat{e}_r\cdot\vec{x}_1}{r}-\frac{\hat{e}_r\cdot\vec{x}_2}{r} \approx 1$$

The approximation used above is the far field approximation. Also needed to find the power are the approximate solutions to the retarded times. Let the phase of the motion be

$$\begin{aligned}\psi_1 &\equiv \omega t_{r1}+\frac{\phi}{2}\\ \psi_2 &\equiv \omega t_{r2}-\frac{\phi}{2}\end{aligned}.$$

The retarded times substituted directly into the phases defined above give

(5.6) $$\begin{aligned}\psi_1 &= \omega\left(t-\frac{r}{c}+\frac{\cos\theta}{c}\left\{-\frac{d}{2}+b\cos(\psi_1)\right\}\right)+\frac{\phi}{2}\\ \psi_2 &= \omega\left(t-\frac{r}{c}+\frac{\cos\theta}{c}\left\{\frac{d}{2}+b\cos(\psi_2)\right\}\right)-\frac{\phi}{2}\end{aligned},$$

very clearly transcendental equations for the two phases. However the coefficient of the $\cos\psi$ term contains the magnitude of the normalized velocity, $\frac{b\omega}{c}$, which is much smaller than 1. Consequently, (5.6) can be approximated as

$$\psi_1 \approx \omega\left(t - \frac{r}{c} - \frac{d\cos\theta}{2c}\right) + \frac{\phi}{2}$$
$$\psi_1 \approx \omega\left(t - \frac{r}{c} + \frac{d\cos\theta}{2c}\right) - \frac{\phi}{2}.$$

This approximation also assumes that the distance between the particles is much larger than the amplitude of oscillation. With this approximation for the phase in (5.1), (5.2) and (5.3), further approximate terms are of interest:

$$\begin{aligned}
\left[\hat{n}_1 \cdot \vec{\alpha}_1\right] &= -\frac{b\omega^2}{c}\cos\left(\psi_1\right)\left\{\cos\theta + \frac{\vec{x}_1 \cdot \hat{e}_z}{r}\cos^2\theta - \frac{\vec{x}_1 \cdot \hat{e}_z}{r}\right\} \\
\left[\hat{n}_2 \cdot \vec{\alpha}_2\right] &= -\frac{b\omega^2}{c}\cos\left(\psi_2\right)\left\{\cos\theta + \frac{\vec{x}_2 \cdot \hat{e}_z}{r}\cos^2\theta - \frac{\vec{x}_2 \cdot \hat{e}_z}{r}\right\} \\
\left[\hat{n}_2 \cdot \vec{\alpha}_1\right] &= -\frac{b\omega^2}{c}\cos\left(\psi_1\right)\left\{\cos\theta + \frac{\vec{x}_2 \cdot \hat{e}_z}{r}\cos^2\theta - \frac{\vec{x}_2 \cdot \hat{e}_z}{r}\right\} \\
\left[\hat{n}_1 \cdot \vec{\alpha}_2\right] &= -\frac{b\omega^2}{c}\cos\left(\psi_2\right)\left\{\cos\theta + \frac{\vec{x}_1 \cdot \hat{e}_z}{r}\cos^2\theta - \frac{\vec{x}_1 \cdot \hat{e}_z}{r}\right\}. \\
\left[\vec{\alpha}_1 \cdot \vec{\alpha}_2\right] &= \frac{b^2\omega^4}{c^2}\cos\left(\psi_1\right)\cos\left(\psi_2\right) \\
\left[\hat{e}_r \cdot \vec{\alpha}_1\right] &= -\frac{b\omega^2}{c}\cos\left(\psi_1\right)\cos\left(\theta\right) \\
\left[\hat{e}_r \cdot \vec{\alpha}_2\right] &= -\frac{b\omega^2}{c}\cos\left(\psi_2\right)\cos\left(\theta\right)
\end{aligned}$$

The electric fields for both particles are

$$\begin{aligned}
\vec{E}_1 &= \frac{q}{4\pi\varepsilon_0 c}\left[\frac{\hat{n}_1\left(\hat{n}_1 \cdot \vec{\alpha}_1\right) - \vec{\alpha}_1}{R_1}\right] \\
\vec{E}_2 &= \frac{q}{4\pi\varepsilon_0 c}\left[\frac{\hat{n}_2\left(\hat{n}_2 \cdot \vec{\alpha}_2\right) - \vec{\alpha}_2}{R_2}\right].
\end{aligned} \tag{5.7}$$

Then the power radiated by each particle separately is found by

(5.8)
$$\begin{aligned} P_1 &= \int r^2 \vec{S}_1 \cdot \hat{e}_r d\Omega \\ P_2 &= \int r^2 \vec{S}_2 \cdot \hat{e}_r d\Omega \end{aligned}.$$

Now add in (5.4) and (5.5) to (5.8) to find

(5.9)
$$\begin{aligned} P_1 &= \frac{1}{\mu_0 c} \int r^2 \left\{ \left|\vec{E}_1\right|^2 + \left(\vec{E}_1 \cdot \vec{E}_2\right) - \left(\hat{e}_r \cdot \vec{E}_2\right)\left(\hat{n}_2 \cdot \vec{E}_1\right) \right\} d\Omega \\ P_2 &= \frac{1}{\mu_0 c} \int r^2 \left\{ \left|\vec{E}_2\right|^2 + \left(\vec{E}_1 \cdot \vec{E}_2\right) - \left(\hat{e}_r \cdot \vec{E}_1\right)\left(\hat{n}_1 \cdot \vec{E}_2\right) \right\} d\Omega \end{aligned}.$$

Combining (5.7) with (5.9) gives

$$P_1 = \frac{q^2}{(4\pi)^2 \varepsilon_0 c} \int r^2 d\Omega \left\{ \begin{array}{l} \dfrac{\alpha_1^2 - \left(\hat{n}_1 \cdot \vec{\alpha}_1\right)^2}{R_1^2} + \\ \dfrac{\left(\hat{n}_1 \cdot \vec{\alpha}_1\right)\left(\hat{n}_2 \cdot \vec{\alpha}_2\right) + \vec{\alpha}_1 \cdot \vec{\alpha}_2 - \left(\hat{n}_1 \cdot \vec{\alpha}_1\right)\left(\hat{n}_1 \cdot \vec{\alpha}_2\right) - \left(\hat{n}_2 \cdot \vec{\alpha}_1\right)\left(\hat{n}_2 \cdot \vec{\alpha}_2\right)}{R_1 R_2} - \\ \dfrac{\left(\hat{n}_2 - \hat{e}_r\right) \cdot \vec{\alpha}_2 \left(\hat{n}_1 - \hat{n}_2\right) \cdot \vec{\alpha}_1}{R_1 R_2} \end{array} \right\}$$

and

$$P_2 = \frac{q^2}{(4\pi)^2 \varepsilon_0 c} \int r^2 d\Omega \left\{ \begin{array}{l} \dfrac{\alpha_2^2 - \left(\hat{n}_2 \cdot \vec{\alpha}_2\right)^2}{R_2^2} + \\ \dfrac{\left(\hat{n}_1 \cdot \vec{\alpha}_1\right)\left(\hat{n}_2 \cdot \vec{\alpha}_2\right) + \vec{\alpha}_1 \cdot \vec{\alpha}_2 - \left(\hat{n}_1 \cdot \vec{\alpha}_1\right)\left(\hat{n}_1 \cdot \vec{\alpha}_2\right) - \left(\hat{n}_2 \cdot \vec{\alpha}_1\right)\left(\hat{n}_2 \cdot \vec{\alpha}_2\right)}{R_1 R_2} - \\ \dfrac{\left(\hat{n}_1 - \hat{e}_r\right) \cdot \vec{\alpha}_1 \left(\hat{n}_2 - \hat{n}_1\right) \cdot \vec{\alpha}_2}{R_1 R_2} \end{array} \right\}.$$

Finally, using Mathematica to integrate and keeping only the terms in the power that have r to the zeroeth order, the results are

$$
\begin{aligned}
P_1 &= P_0 \cos^2\left(\omega t - \frac{\omega r}{c}\right)\left\{1 - 3\left(\cos\phi - \sin\phi \tan\left(\omega t - \frac{\omega r}{c}\right)\right)\left(\frac{\cos\left(\frac{\omega d}{c}\right)}{\left(\frac{\omega d}{c}\right)^2} - \frac{\sin\left(\frac{\omega d}{c}\right)}{\left(\frac{\omega d}{c}\right)^3}\right)\right\} \\
P_2 &= P_0 \cos^2\left(\omega t - \frac{\omega r}{c}\right)\left\{1 - 3\left(\cos\phi + \sin\phi \tan\left(\omega t - \frac{\omega r}{c}\right)\right)\left(\frac{\cos\left(\frac{\omega d}{c}\right)}{\left(\frac{\omega d}{c}\right)^2} - \frac{\sin\left(\frac{\omega d}{c}\right)}{\left(\frac{\omega d}{c}\right)^3}\right)\right\}
\end{aligned}
\tag{5.10}
$$

where $P_0 = \frac{\mu_0 b^2 q^2 \omega^4}{6\pi c}$ is the peak power radiated by a single point charge. The result appears to depend on the imaginary surface where the fields were evaluated because of the dependence on r. However, the r dependence can be suppressed by redefining the time as $\tau \equiv t - \frac{r}{c}$. This time can be interpreted as the time that is retarded to the center of the imaginary surface and coincides with the center of the charge distribution. Because the problem is non-relativistic, the issue of simultaneity does not appear and the redefinition of time means that the powers in (5.10) are now to be interpreted as instantaneous radiated powers rather than as the power that passes through the imaginary surface. With further definitions (5.10) can be rewritten as

$$
\begin{aligned}
P_1 &= P_0 \cos^2\tau\left\{1 - 3F(u)\cos\phi + 3F(u)\sin\phi\tan\tau\right\} \\
P_2 &= P_0 \cos^2\tau\left\{1 - 3F(u)\cos\phi - 3F(u)\sin\phi\tan\tau\right\},
\end{aligned}
\tag{5.11}
$$

where $F(u) \equiv \frac{\cos u}{u^2} - \frac{\sin u}{u^3}$ and $u \equiv \frac{\omega d}{c}$. This result is only good when the motion of the charges is non-relativistic and the distance between the charges is much larger than the amplitude of oscillations. The total power is the sum of the two terms in (5.11), again the sum can only be taken because the relativistic issue of simultaneity does not occur,

(5.12) $$P = P_1 + P_2 = 2P_0 \cos^2 \tau \left\{1 - 3F\left(u\right)\cos\phi\right\}.$$

The coherence in the power depends on the distance between the particles and their relative phase. The plot in Figure 14 shows the normalized power of both particles plotted as a function of u, where $\phi = \frac{\pi}{3}$ and $\tau = 3$ were chosen. Because of the chosen phase and time the plot does not show complete coherence. As u increases the normalized power approaches a value that is a little smaller than 2, it would be exactly 2 if $\cos\tau = 1$, this is the incoherent limit where the 2 point charges radiate independently of each other. As u goes to zero the normalized power approaches a value that is a little smaller than 3, it would be exactly 4 if $\cos\tau = 1$ and $\phi = 0$, this is the completely coherent limit where the power is enhanced by N^2. The approximation $d \gg b$ places a limit on d which places a limit on u. However, b can be made very small so that u can be made very small and the graph will be valid for smaller values of u. The amplitude of oscillations affects the amplitude of the electric field, $\left|\vec{E}\right| \propto b\omega^2$, and so will have a lower limit imposed by quantum mechanics. At the same time ω also affects the amplitude so that b can be decreased at the same time that ω is increased, but slower than b, in order to prevent the amplitude of the electric field from becoming too small. In this way u

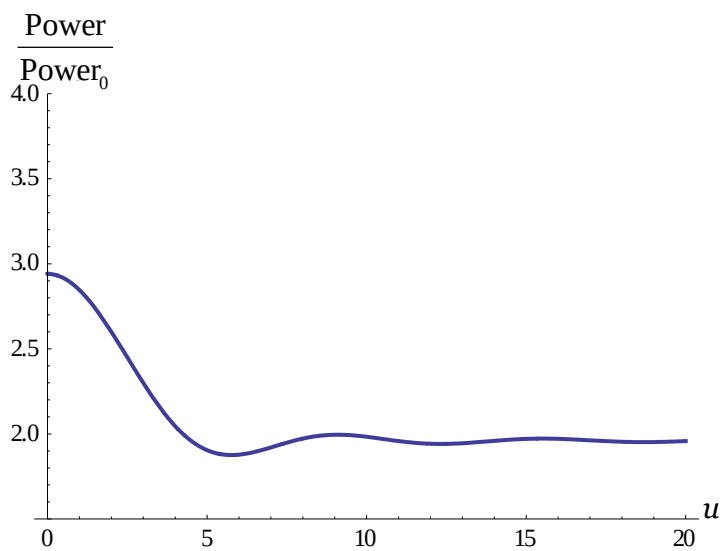

Figure 14: The normalized power of two particles versus the dimensionless distance.

can be made as small as necessary to validate the figure. A very similar dependence has been found by [1] , using the modified Feynman-Wheeler Absorber theory [3].

Appendix I: Experimental Work on Coherent THz Radiation

The Mark III FEL at the University of Hawai'i at Manoa has a roughly 40 MeV electron beam that is bunched with pulse lengths of about 1 ps. The short pulse lengths and high number of electrons per pulse ($\sim 10^9$) provide a good opportunity of observing coherent radiation at THz frequencies. The transition from coherent to incoherent radiation is dictated by the pulse length and for a 1 ps pulse length occurs at $f = \frac{1}{1\text{ ps}} = 10^{12}\text{ Hz} = 1\text{ THz}$. As a result, experimental measurements of the coherent to incoherent transition are a rough measure of the pulse length of the bunch and a good diagnostic for the electron beam. [5]

There are two possibilities; transition radiation, or synchrotron radiation. This section evaluates the feasibility of doing further experimental work to examine the coherent radiation at THz frequencies and using the measured radiation as a diagnostic for the electron beam. The transition radiation was measured directly with a pyroelectric detector to discover if there was sufficient power to use an interferometer to measure the radiated power as a function of the frequency. The synchrotron radiation was modeled theoretical to estimate the power that would be radiated for the same purpose.

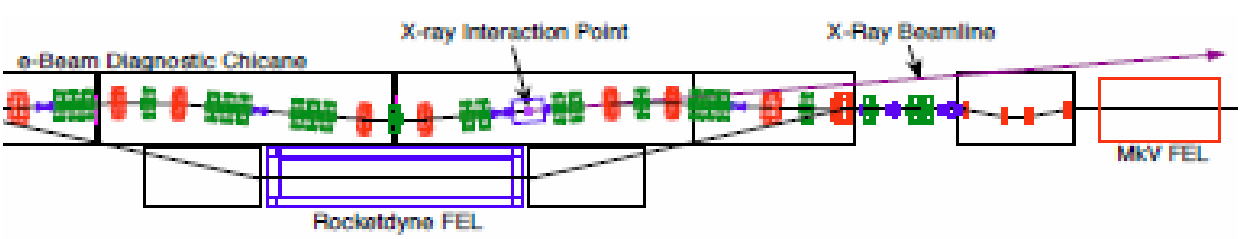

Figure 15: The beam line; with the transition radiation generated at the X-ray interaction point, and the synchrotron radiation proposed for just before the MkV FEL.

Synchrotron radiation

The bunched electron beam is transported through many dipole and quadrupole magnets. The synchrotron radiation will be highest in the dipole magnet with the strongest magnetic field. A single electron that enters the dipole will be deflected in a circular orbit. Let the deflection angle of the electron be ψ, in order to parameterize the orbit. Let θ be the observation angle with respect to the plane of deflection. Then the power radiated by a single electron per deflection angle per observation angle is

$$\frac{\partial^2 P}{\partial\psi\partial\theta} = \frac{21}{32}\frac{P_\gamma}{2\pi}\frac{\gamma}{(1+\gamma^2\theta^2)^{5/2}}\left[1+\frac{5}{7}\frac{\gamma^2\theta^2}{1+\gamma^2\theta^2}\right].$$

The first term in the square brackets corresponds to the σ-mode and the second term to the π-mode. [12] The P_γ is the Liénard power for a single electron

$$P_\gamma = \frac{cC_\gamma E(GeV)^4}{2\pi\rho^2},$$

where $C_\gamma = 8.8460\times10^{-5}\frac{m}{(GeV)^3}$ and $\rho = \frac{\beta E}{ceB}$ is the radius of the circular orbit which depends on the speed(βc), energy(E), charge(e), and magnetic field(B). [12] The power radiated into the two modes is distributed differently with respect to θ. The σ-mode radiates much more closely to the plane of deflection than the π-mode. The total amount of instantaneous power radiated into each mode is

$$P_\sigma = \frac{7}{8}P_\gamma \quad P_\pi = \frac{1}{8}P_\gamma .$$

Alternatively, the synchrotron radiated power from a single electron can be expressed in terms of the photon flux, i.e. number of photons per second. [12] The critical photon energy defines the critical frequency

$$\omega_c = \frac{3c\gamma^3}{2\rho}.$$

Then the total photon flux per unit deflection angle for beam current I [12] is

(6.1) $$\frac{d\dot{N}_{ph}}{d\psi} = C_\psi E(GeV) I \frac{\Delta\omega}{\omega} S(\frac{\omega}{\omega_c})$$

Where $C_\psi = 3.9614 \times 10^{19} \frac{\text{photons}}{\text{s rad A GeV}}$ and

$$S(\frac{\omega}{\omega_c}) = \frac{9\sqrt{3}}{8\pi} \frac{\omega}{\omega_c} \int_{\omega/\omega_c}^{\infty} K_{5/3}(x)dx.$$

The beam parameters for the Mark III FEL:

$$E = 40 \text{ MeV}$$

$$I_{peak} = 30 \text{ Amps}$$

$$\frac{\Delta\omega}{\omega} = 1\%$$

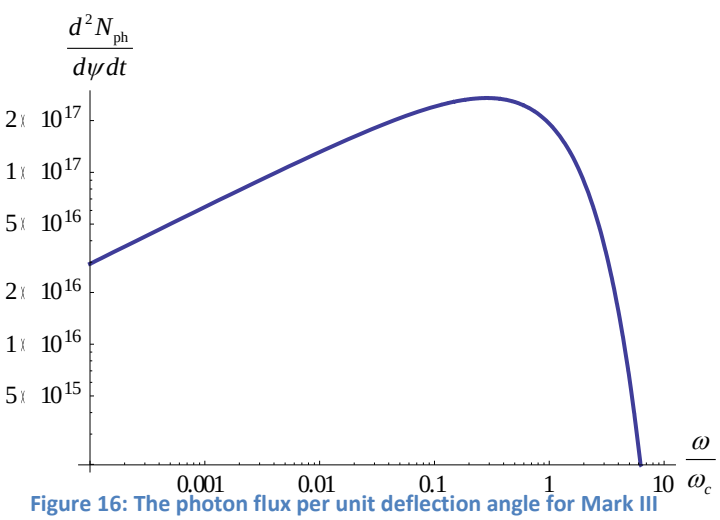

Figure 16: The photon flux per unit deflection angle for Mark III parameters.

With these parameters, figure 15 shows the spectral distribution of photons per second per deflection angle. This indicates that there will not be very much power radiated for frequencies higher than $10\omega_c$. Also, due to shielding caused by the dimensions of

the pipe, radiation with a wavelength $\lambda \geq$ pipe dimensions will not form, which causes a lower limit on the radiation frequency. For a 1" diameter pipe the cutoff frequency is

$\omega_{\text{cut}} = 7.42 \times 10^{10} \ \frac{\text{rad}}{\text{sec}}$.

For an estimate of the power, the following beam parameters are also included: 70 pC per bunch; a bunch length of 1 pSec; one bunch occurring every 350 pSec; and a macro-pulse length of 4 μSec. The number of electrons in a micro-pulse is then 4.375 x 10^8. For the worst case scenario, incoherent radiation, the average incoherent power during the macro-pulse is

$$\bar{P}_{inc} = N_e P_\gamma \left(\frac{1 \text{ ps}}{350 \text{ ps}} \right).$$

Assuming a bending radius of $\rho = 0.266$ meter which corresponds to a magnetic field of 0.5 Tesla, then the average incoherent power radiated during the macro-pulse is

$$\bar{P}_{inc} = 30.5 \ \mu\text{W}.$$

For the best case scenario, coherent radiation, the average coherent power radiated during the macro-pulse is

$$\bar{P}_{coh} = N_e^2 P_\gamma \left(\frac{1 \text{ ps}}{350 \text{ ps}} \right).$$

With the same assumption for the bending radius then the average coherent power radiated during the macro-pulse is

$$\bar{P}_{coh} = 13.3 \text{ kW}.$$

This is unrealistically high due to the cutoff frequency from the pipe and the partial coherence that will occur only for wavelengths larger than the length of the micro-pulse.

The critical frequency is $\omega_c = 8.34\times10^{14}\ \frac{\text{rad}}{\text{sec}}$, the visible spectrum starts at $2.7\times10^{15}\ \frac{\text{rad}}{\text{sec}}$. So the critical frequency is in the near infrared. The condition on coherence requires that the wavelength of coherent light be longer than the bunch length of the charge so the frequency must be smaller than $6.28\times10^{12}\ \frac{\text{rad}}{\text{sec}}$.

Another way to estimate the radiated power is to look at the energy density in the magnetic field times the speed of light times the Thomson cross section to get an estimate of the power radiated by a single electron [13]

$$P_\gamma = (9.9\times10^4\ \frac{\text{eV}}{\text{s}})\left(\frac{B}{1\ \text{T}}\right)^2 \gamma^2 .$$

The magnetic field is found from $B = \frac{\beta E}{ce\rho}$ where $\beta \approx 1$ then $B = 0.5\ \text{T}$. Then with this magnetic field the power from a single electron is

$$P_\gamma = 1.54\times10^8\ \frac{\text{eV}}{\text{s}} = 2.47\times10^{-11}\ \text{W},$$

and multiplying by the duty cycle and the number of electrons gives the incoherent power

$$\bar{P}_{inc} = 30.9\ \mu\text{W}.$$

This is almost the same as the previous estimate of 30.5 μW. The idealized coherent power over the 4 μ sec pulse length gives 53.2 mJ of energy radiated.

After radiating the light must reflect off of mirrors with energy losses as well as transmit through a window also with energy losses. The transmission loss through the crystal quartz

window is about 20% for a wide range of frequencies. The reflection loss at the mirrors would add a few more % to the energy loss. Estimating 30% energy loss from the mirrors and window seems reasonable. The radiation also is diverging from the axis and could be lost from the detector due to the finite detector size. Since 7/8 of the power is radiated in the σ-mode and that is the mode that will be close to the axis, another factor of 1/8 should be taken off of the energy. The energy impinging on the detector from the case of idealized coherent emission is

$$E \approx \left(\frac{7}{8}\right)\left(\frac{7}{10}\right) 53.2 \text{ mJ} = 32.6 \text{ mJ} .$$

The detector itself has an efficiency that depends on frequency that can affect the measured energy radiated, although it is unclear to me whether or not the detector takes this into account.

The amplified pyroelectric detector (J4-09) which has a voltage responsivity of 0.8 V per mJ will be able to detect the coherent synchrotron radiation but not the incoherent synchrotron radiation. Because of this the detectable radiated power should be in the frequency range from $7.42\times10^{10}\ \frac{\text{rad}}{\text{sec}}$ to $6.28\times10^{12}\ \frac{\text{rad}}{\text{sec}}$. Also the electrical decay time of the detector is 2 msec, therefore the detector will integrate the signal over the 4 μ sec macro-pulse. But it should detect separately the next macro-pulse that comes by 0.2 sec later. Synchrotron radiation will be usable to estimate the bunch length of the pulse.

Transition radiation

In addition to synchrotron radiation the Mark III diagnostic chicane is setup to create transition radiation. Copper plates can be placed in the beam line and brehemstralung and transition radiation will be produced and directed out of the ports in the beam line. At the x-ray interaction point, measurements of the transition radiation were made with no filter and a J4-09 amplified pyroelectric detector. The detector was placed right up against the crystal quartz

window of the beam line port. Data was taken with the e-beam passing by the port with no plate in place to create transition radiation, then with the plate in place. Then data was taken with the beam stop in place preventing the e-beam from reaching the copper plate, then with the beam stop out so that the e-beam was hitting the copper plate. The same procedure was repeated again with Aluminum foil (folded once) placed between the quartz window and the detector. The oscilloscope trace was also optimized by adjusting the e-beam parameters. The transition radiation was sensitive to bunch length, quad focusing, and small changes in the phase.

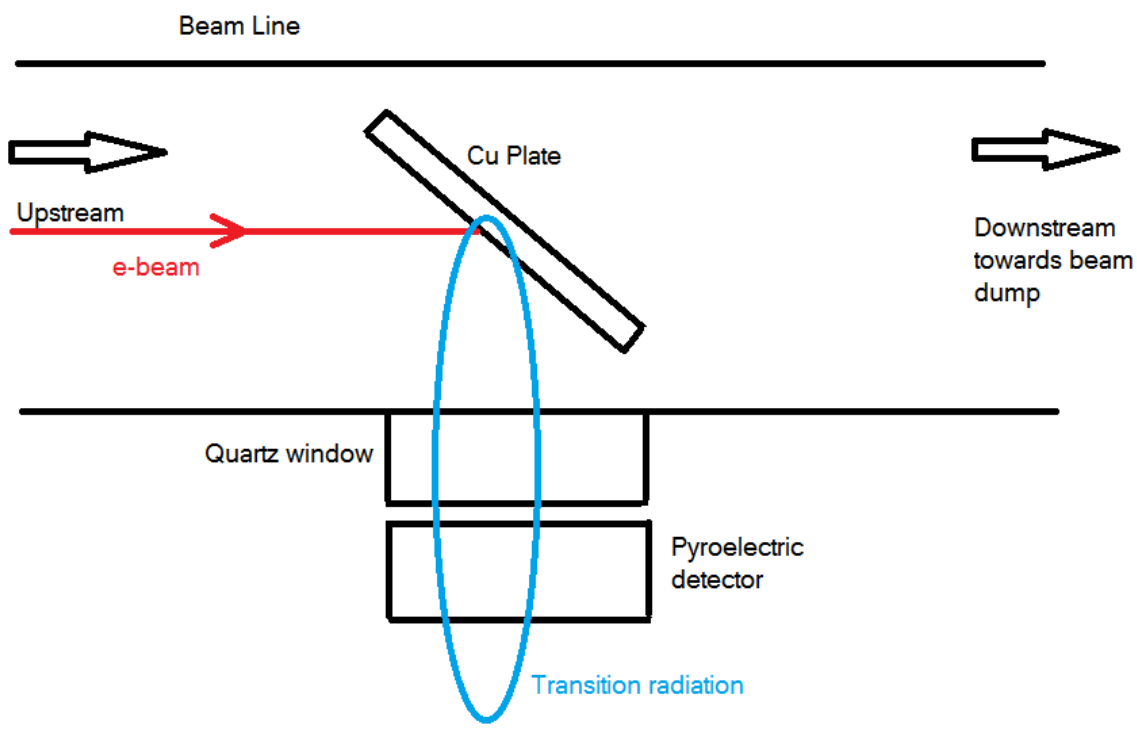

Figure 17: Diagram of the generation and measurement of transition radiation. The pyroelectric detector was placed as close to the quartz window as possible.

The oscilloscope data was then analyzed by subtracting the peak of the optimized signal from the reference signal. With the Aluminum foil in place the lower frequencies are blocked but the ionizing radiation is still getting through. So a comparison of the optimized peak with the peak from when the Aluminum foil was in place will give the signal due to the transition

radiation. The peak voltage measured with the foil was 0.0068 V. The peak voltage measured with the optimized setup and no foil was 0.0194 V. So the detected transition radiation was 0.0126 V, which corresponds to 15.75 μJ when the voltage responsivity is used.

In conclusion, either the transition radiation or the synchrotron radiation could be used to make measurements of the bunch length of the electron beam. The synchrotron radiation would give a non-destructive measure of the bunch length, while the transition radiation requires that the e-beam be destroyed. The synchrotron radiation method could measure the bunch length at the same time as the e-beam lases in the undulator, and would be a preferable diagnostic for the bunch length.

Appendix 2: The Wave Equation

For the Appendix, there are two goals. 1) The concepts of retarded and advanced fields are to be introduced. 2) The Fourier transform is to be applied to (7.1) and (7.2) in order to find the unbounded Green functions of the potentials, and then the solutions are to be compared to the solutions found by the same method of (7.3).

Electromagnetism is encapsulated in Maxwell's equations for the electric and magnetic fields, in vacuum and SI units these are

$$\begin{aligned} \nabla\cdot\vec{E} &= \frac{\rho}{\varepsilon_0} & \nabla\times\vec{E} &= -\frac{\partial\vec{B}}{\partial t} \\ \nabla\cdot\vec{B} &= 0 & \nabla\times\vec{B} &= \mu_0\vec{J} + \mu_0\varepsilon_0\frac{\partial\vec{E}}{\partial t} \end{aligned}.$$

Where $\vec{E}$ is the electric field, ρ is the volume charge density, $\varepsilon_0 = 8.85\times10^{-12}$ F/m is the permittivity of free space, $\vec{B}$ is the magnetic field, $\vec{J}$ is the volume current density, and $\mu_0 \equiv 4\pi\times10^{-7}$ H/m is the permeability of free space. According to the Helmholtz theorem, a vector field is uniquely defined if both the divergence and curl of that vector field is known. Maxwell's equations are coupled in the sense that the curl of one field depends on the time derivative of the other field. In order to simplify the mathematics, potentials are introduced that automatically satisfy two of Maxwell's equations. The vector potential is defined, $\vec{B}\equiv\nabla\times\vec{A}$, to satisfy Gauss's Law for the magnetic field

$$\nabla\cdot\vec{B} = \nabla\cdot(\nabla\times\vec{A}) = 0.$$

Then using this definition for the vector potential in Faraday's Law

$$\nabla \times \vec{E} + \frac{\partial \vec{B}}{\partial t} = \nabla \times \left(\vec{E} + \frac{\partial \vec{A}}{\partial t} \right) = 0$$

allows for the definition of a scalar potential such that $\vec{E} \equiv -\nabla\Phi - \frac{\partial \vec{A}}{\partial t}$. The remaining two equations of Maxwell's equations are then expressed in terms of the potentials. Coulomb's law becomes

(7.1) $$-\nabla^2\Phi - \frac{\partial}{\partial t}\nabla \cdot \vec{A} = \frac{\rho}{\varepsilon_0}$$

and Ampere's law becomes

(7.2) $$\nabla \times \left(\nabla \times \vec{A} \right) = \mu_0 \vec{J} - \frac{\partial}{c^2 \partial t}\nabla\Phi - \frac{\partial^2 \vec{A}}{c^2 \partial t^2}.$$

There is a vector identity for the curl of a curl, $\nabla \times (\nabla \times \vec{A}) \rightarrow \nabla(\nabla \cdot \vec{A}) - \nabla^2 \vec{A}$ that is only valid for Cartesian coordinates. Curvilinear coordinates such as cylindrical or spherical coordinates cannot use that identity. However, if this identity is used, then the inhomogeneous wave equation can be expressed as

(7.3) $$\begin{aligned} \left[\nabla^2 - \frac{1}{c^2}\frac{\partial^2}{\partial t^2} \right]\Phi + \frac{\partial}{\partial t}\left[\nabla \cdot \vec{A} + \frac{1}{c^2}\frac{\partial \Phi}{\partial t} \right] &= -\frac{\rho}{\varepsilon_0} \\ \left[\nabla^2 - \frac{1}{c^2}\frac{\partial^2}{\partial t^2} \right]\vec{A} + \frac{\partial}{\partial t}\left[\nabla \cdot \vec{A} + \frac{1}{c^2}\frac{\partial \Phi}{\partial t} \right] &= \mu_0 \vec{J} \end{aligned}.$$

These equations are manifestly covariant, i.e. the equations respect special relativity. Consequently, fields found from (7.3) are considered valid even if they are found with a curvilinear coordinate system. The issue with curvilinear coordinates has been noticed but largely ignored. [6]

In order to solve (7.1) and (7.2), the same standard method of solution that is applied to the inhomogeneous wave equation, (7.3), will be used. The solutions found will be the unbounded Green function solutions for the differential equations. By defining the symmetric Fourier transform in both time and space as

$$\vec{A}(\vec{r},t)=\frac{1}{(2\pi)^2}\int_{\text{All freq}}\vec{A}_k(\vec{k},\omega)e^{i\left(\vec{k}\cdot\vec{r}-\omega t\right)}d^3k\,d\omega\,.$$

Then the equations for the Fourier coefficients are found by substituting $\nabla\to i\vec{k}$ and $\frac{\partial}{\partial t}\to -i\omega$. Coulomb's Law, (7.1), becomes

(7.4) $$k^2\Phi_k-\omega\vec{k}\cdot\vec{A}_k=\frac{\rho_k}{\varepsilon_0}$$

and Ampere's law, (7.2), becomes

(7.5) $$-\vec{k}\times(\vec{k}\times\vec{A}_k)=\mu_0\vec{J}_k-\frac{1}{c^2}\omega\vec{k}\Phi_k+\frac{\omega^2}{c^2}\vec{A}_k\,.$$

Now solve Coulomb's law for Φ_k,

$$\Phi_k=\frac{\rho_k}{k^2\varepsilon_0}+\frac{\omega}{k^2}\vec{k}\cdot\vec{A}_k$$

and substitute it into (7.5)

$$-\vec{k}\times(\vec{k}\times\vec{A}_k)=\mu_0\vec{J}_k+\frac{\omega^2}{c^2}\vec{A}_k-\frac{\omega}{c^2}\vec{k}\left\{\frac{\rho_k}{k^2\varepsilon_0}+\frac{\omega}{k^2}\vec{k}\cdot\vec{A}_k\right\}.$$

The bac-cab rule can be used, even in curvilinear coordinates, so that the above equation is

(7.6) $$\vec{k}(\vec{k}\cdot\vec{A}_k)-k^2\vec{A}_k=-\mu_0\vec{J}_k+\frac{\omega\rho_k}{c^2\varepsilon_0}\frac{\vec{k}}{k^2}-\frac{\omega^2}{c^2}\vec{A}_k+\frac{\omega^2}{c^2}\frac{\vec{k}(\vec{k}\cdot\vec{A}_k)}{k^2}\,.$$

Let $\vec{A}_k = \vec{A}_{\|} + \vec{A}_{\perp}$, where $\|$ and $\perp$ are with respect to $\vec{k}$ in frequency space. Then (7.6) can be decomposed into two equations for the two orientations with respect to $\vec{k}$. The parallel components give the law of charge conservation

$$0 = \frac{\omega\rho_k}{c^2\varepsilon_0}\frac{\vec{k}}{k^2} - \mu_0\vec{J}_{\|} \rightarrow \nabla\cdot\vec{J} = -\frac{\partial\rho}{\partial t}.$$

The perpendicular components give an expression for $\vec{A}_{\perp}$

(7.7) $$-k^2\vec{A}_{\perp} = -\mu_0\vec{J}_{\perp} - \frac{\omega^2}{c^2}\vec{A}_{\perp} \rightarrow \vec{A}_{\perp} = \frac{\mu_0\vec{J}_{\perp}}{k^2 - \frac{\omega^2}{c^2}}.$$

The parallel component of the vector potential cancels out completely in(7.6), this should be interpreted as gauge freedom. The electric and magnetic fields can be found from the definitions for the potentials, so that in frequency space

$$\begin{aligned}\vec{E}_k &= -i\vec{k}\Phi_k + i\omega\vec{A}_k \\ \vec{B}_k &= i\vec{k}\times\vec{A}_k\end{aligned}.$$

The magnetic field depends only on $\vec{A}_{\perp}$, as does the electric field which can be seen by substituting for Φ_k.

$$\vec{E}_k = -i\vec{k}\left(\frac{\rho_k}{k^2\varepsilon_0} + \frac{\omega}{k^2}kA_{\|}\right) + i\omega\vec{A}_{\perp} + i\omega\vec{A}_{\|}$$

the last term is canceled by the second term so that both fields depend only on $\vec{A}_{\perp}$

$$\begin{aligned}\vec{E}_k &= -i\vec{k}\frac{\rho_k}{k^2\varepsilon_0} + i\omega\vec{A}_{\perp} \\ \vec{B}_k &= i\vec{k}\times\vec{A}_{\perp}\end{aligned}.$$

Choosing a gauge completely defines the potentials, for example the Coulomb gauge when transformed to frequency space is

(7.8) $$\nabla \cdot \vec{A} = 0 \rightarrow i\vec{k} \cdot \vec{A}_k = 0 \rightarrow \vec{A}_{\|} = 0$$

With this gauge the potentials are given by

(7.9) $$\begin{aligned} \Phi_k &= \frac{\rho_k}{k^2 \varepsilon_0} \\ \vec{A}_k &= \frac{\mu_0 \vec{J}_{\perp}}{k^2 - \frac{\omega^2}{c^2}} \end{aligned} .$$

These results are identical to the results found by using (7.3) with(7.8). [6] Choosing a different gauge, such as the Lorenz gauge, will change the potentials but not the fields. The Lorenz gauge is, when transformed to frequency space,

(7.10) $$\nabla \cdot \vec{A} + \frac{1}{c^2}\frac{\partial \Phi}{\partial t} = 0 \rightarrow i\vec{k} \cdot \vec{A}_k - \frac{i\omega}{c^2}\Phi_k = 0 .$$

Substituting the Lorenz gauge into the scalar potential gives

$$\Phi_k = \frac{\rho_k}{k^2 \varepsilon_0} + \frac{\omega^2}{c^2 k^2}\Phi_k \rightarrow \Phi_k = \frac{\rho_k}{\varepsilon_0\left(k^2 - \frac{\omega^2}{c^2}\right)} .$$

The transverse vector potential is gauge independent, but the longitudinal vector potential is now non zero and found from (7.10) and charge conservation. Multiply (7.10) by $\vec{k}$ to get

$$\left(k^2 - \frac{\omega^2}{c^2}\right)\vec{k}(\vec{k} \cdot \vec{A}_k) = \frac{\omega \rho_k}{c^2 \varepsilon_0}\vec{k} = \mu_0 k^2 \vec{J}_{\|} .$$

This gives an expression for $\vec{A}_{\|}$

$$\vec{A}_{\|} = \frac{\mu_0 \vec{J}_{\|}}{k^2 - \frac{\omega^2}{c^2}}$$

that can be combined with (7.7) to give an expression for the complete vector potential, such that the potentials are found from

$$\begin{aligned} \Phi_k &= \frac{\rho_k}{\varepsilon_0 (k^2 - \frac{\omega^2}{c^2})} \\ \vec{A}_k &= \frac{\mu_0 \vec{J}_k}{k^2 - \frac{\omega^2}{c^2}} \end{aligned} \quad . \tag{7.11}$$

This is identical to the solutions found from (7.3) with the gauge condition(7.10). [6] In the frequency domain and unbounded space, the solutions of (7.1) and (7.2) are identical to the solutions of (7.3) so long as the same gauge condition is respected in both cases.

In curvilinear coordinate systems the differential equations given by (7.1) and (7.2) are different from the differential equations given by (7.3). However, the eigenvectors for these differential equations are the same, suggesting that the vector identity

$$\nabla \times \left(\nabla \times \vec{A} \right) = \nabla \left(\nabla \cdot \vec{A} \right) - \nabla^2 \vec{A}$$

is effectively valid for curvilinear coordinate systems when dealing with potentials in classical electromagnetism. The validity of this vector identity has only been explored for the vector potential, not the electric and magnetic fields.

The inverse Fourier transforms must be taken of (7.9) or (7.11) in order to find the time domain and space coordinate unbounded particular solutions for the potentials. This requires a contour integral because of the poles that are present on the real axis. The choice of contour has physical implications for the solutions. Traditionally, the contour is chosen to impose causality,

the solutions that are causal are called retarded solutions. Causal means that the cause precedes, in time, the effect. For retarded solutions, at the field point, the electric and magnetic field will depend on the source at an earlier time, called the retarded time, which depends on the distance of the field point to the source at the retarded time. The source is thought to have emitted the fields at the retarded time and then propagated the fields at the speed of light to the field point. An alternate choice of the contour will not impose causality; these solutions are called advanced solutions. For the advanced solutions the source emits at a future time, the advanced time, which depends on the distance from the field point to the source at the advanced time. In this case the fields propagate at the speed of light backwards in time. All experiments that I know of are consistent with the concept of causality, consequently it is standard to dispose of the advanced solutions and use only the retarded solutions.

Conclusions

The work presented here has a fundamental restructuring of the unique assignment of radiated power to systems of particles that has many applications beyond the Kimel-Elias approach. The examples of the Kimel-Elias approach that were worked in chapter 4 should provide sufficient knowledge of the approach that computer simulations of more realistic problems can be done in the future. The application of the partial power to a non-relativistic example as well as the general agreement the retarded theory had with the Feynman-Wheeler Absorber theory are new developments in classical electromagnetism.

Future Work

In the future, work can be done to include finite emittance and energy spread in the Kimel-Elias approach. Then simulations can be done for SASE radiation and FEL startup. Adding conducting boundary conditions could possibly be accomplished with the introduction of image charges.

Experimental measurements of transition and synchrotron radiation from the Mark III FEL to determine the bunch length and to examine in detail the transition from coherent to incoherent radiation. A detector that could make measurements of the pulses with single pulse capability and sufficient resolution would greatly aid this effort.

List of Possible Publications

Possible publications that could be derived from this work are

1. The evaluation and limitations of the Kimel-Elias approach to multiple point charge radiation reaction.

2. The radiation reaction for two non-relativistic dipole radiators using retarded time integrals of the Poynting vector in relation to existing work on the same problem using the Feynman-Wheeler Absorber theory.

Bibliography

[1] P. Niknejadi, J. M. J. Madey and J. M. D. Kowalczyk, "Energy Conservation of Coherently Oscillating Charged Particles in Classical Electrodynamics," *Physical Review D.,* submitted Aug. 2014.

[2] P. A. M. Dirac, "Classical Theory of Radiating Electrons," in *Proceedings of the Royal Society of London. Series A, Mathematical and Physical Sciences*, London, 1938.

[3] R. P. Feynman and J. Wheeler, "Interaction with the Absorber as the Mechanism of Radiation," *Reviews of Modern Physics,* vol. 17, pp. 157-181, 1945.

[4] I. Kimel and L. Elias, "Coherent Radiation Reaction in Free-Electron Sources," *Physical Review Letters,* vol. 75, no. 23, pp. 4210-4213, 1995.

[5] H. Lihn, P. Kung, C. Settakorn and H. Wiedemann, "Measurement of subpicosecond electron pulses," *Physical Review E,* vol. 53, no. 6, pp. 6413-6418, 1996.

[6] A. Zangwill, Modern Electrodynamics, New York: Cambridge University Press, 2013.

[7] S. Parrott, Relativistic Electrodynamics and Differential Geometry, New York: Springer-Verlag, 1987.

[8] F. Rohrlich, Classical Charged Particles, Singapore: World Scientific Publishing Co., 2007.

[9] W. K. H. Panofsky and M. Phillips, Classical Electricity and Magnetism, Mineola: Dover Publications, Inc., 2005.

[10] A. Bajo, I. Dymnikova, A. Sakharov, E. U. J. Sanchez and J. Zhao, "Quantum Electrodynamics and Physics of the Vacuum," *AIP Conference Proceeding,* vol. 564, pp. 255-262, 2001.

[11] E. B. Szarmes, ""Classical Theory of Free-Electron Lasers", Lecture Notes," September 2013. [Online]. Available: http://www.phys.hawaii.edu/~szarmes/FELnotes.v400.pdf.

[12] H. Wiedemann, in *Handbook of Accelerator Physics and Engineering*, World Scientific Publishing, 1999.

[13] G. Pollack and D. Stump, Electromagnetism, San Francisco: Addison Wesley, 2002.